

2

AD-A238 158

AFOSR-TR- 91 06 21



A STUDY OF THE BEHAVIOR AND MICROMECHANICAL MODELLING OF GRANULAR SOIL

VOLUME III

A NUMERICAL INVESTIGATION OF THE BEHAVIOR OF GRANULAR MEDIA USING NONLINEAR DISCRETE ELEMENT SIMULATIONS

by

Emmanuel Petrakis  
Ricardo Dobry  
Tang-Tat Ng

and  
Li Liu

Approved for public release; Distribution Unlimited.

AIR FORCE  
OFFICE OF SCIENTIFIC RESEARCH  
BOLLING AIR FORCE BASE  
WASHINGTON, D.C. 20330-3901  
AFOSR-TR-91-06-21  
15 JUL 1991  
DISTRIBUTION STATEMENT A  
Approved for public release; Distribution Unlimited.

Prepared under Contract No. AFOSR-89-0350  
United States Air Force  
Office of Scientific Research  
Bolling Air Force Base

Department of Civil Engineering  
Rensselaer Polytechnic Institute  
Troy, NY 12180-3590

May 1991

DISTRIBUTION STATEMENT A  
Approved for public release;  
Distribution Unlimited

91-04782



91 7 11 076

REPORT DOCUMENTATION PAGE			Form Approved OMB No. 0704-0188
<small>Public reporting burden for this collection of information is estimated to average 1 hour per response, including the time for reviewing instructions, searching existing data sources, gathering and maintaining the data needed, and completing and reviewing the collection of information. Send comments regarding this burden estimate or any other aspect of this collection of information, including suggestions for reducing this burden, to Washington Headquarters Services, Directorate for Information Operations and Reports, 1215 Jefferson Davis Highway, Suite 1204, Arlington, VA 22202-4302, and to the Office of Management and Budget, Paperwork Reduction Project (0704-0188), Washington, DC 20503.</small>			
1. AGENCY USE ONLY (Leave blank)	2. REPORT DATE May 22, 1991	3. REPORT TYPE AND DATES COVERED Final 1/6/89-5/15/91	
4. TITLE AND SUBTITLE A Study of the Behavior and Micromechanical Modelling of Granular Soil <i>Volume 3</i>		5. FUNDING NUMBERS Grant AFOSR-89-0350 PR 2302/C1	
6. AUTHOR(S) Emmanuel Petrakis, Ricardo Dobry, Paul Van Laak, Panos Kotsanopoulos, Tang-Tat Ng, and Li Liu			
7. PERFORMING ORGANIZATION NAME(S) AND ADDRESS(ES) Civil Engineering Department Rensselaer Polytechnic Institute Troy, NY 12180-3590		8. PERFORMING ORGANIZATION REPORT NUMBER	
9. SPONSORING/MONITORING AGENCY NAME(S) AND ADDRESS(ES) AFOSR/NA Bldg. 410 Bolling AFB Washington, DC 20332-6448		10. SPONSORING/MONITORING AGENCY REPORT NUMBER <i>AFOSR-89-0350</i>	
11. SUPPLEMENTARY NOTES			
12a. DISTRIBUTION/AVAILABILITY STATEMENT Approved for Public Release; Distribution Unlimited		12b. DISTRIBUTION CODE	
13. ABSTRACT (Maximum 200 words) <p>A comprehensive research effort has been conducted on constitutive and micromechanical modelling of granular soil. This includes: 1) the development of a new constitutive relation for granular media based on the contact law between two spheres; 2) an experimental investigation on the stress-strain response of a glass bead material with 46 monotonic and cyclic experiments on hollow cylinder specimens, most of them constant mean stress tests to measure deviatoric response and behavior of initial and subsequent yield loci; and 3) numerical simulations of the behavior of granular media using the discrete element method.</p> <p>The proposed constitutive law captures a number of key aspects of the observed stress-strain behavior of granular soils, and it predicts well the experiments on glass beads. Novel aspects of the proposed model include yield cones parallel to the failure envelope, and a basic relation between the field of elastoplastic moduli and the elastic constants of the material.</p>			
14. SUBJECT TERMS Micromechanics; Constitutive Law; Granular Media; Sand; Yield Surface Distortion; Hollow Cylinder Experiment; Discrete Element Simulations; Plasticity		15. NUMBER OF PAGES	
		16. PRICE CODE	
17. SECURITY CLASSIFICATION OF REPORT Unclassified	18. SECURITY CLASSIFICATION OF THIS PAGE Unclassified	19. SECURITY CLASSIFICATION OF ABSTRACT Unclassified	20. LIMITATION OF ABSTRACT UL

The report consists of three volumes, as follows:

Volume I: "A Constitutive Law for Granular Materials Based on the Contact Law Between Two Spheres," by R. Dobry and E. Petrakis.

Volume II: "An Experimental Investigation of the Behavior of Granular Media Under Load," by E. Petrakis, R. Dobry, P. Van Laak, and P. Kotsanopoulos.

Volume III: "A Numerical Investigation of the Behavior of Granular Media Using Nonlinear Discrete Element Simulations," by E. Petrakis, R. Dobry, T.-T. Ng, and L. Liu.

## TABLE OF CONTENTS

	page
ACKNOWLEDGEMENTS .....	1
ABSTRACT .....	2
1. INTRODUCTION .....	3
1.1 General .....	3
1.2 Studies on Polycrystalline Aggregates .....	4
1.3 Modelling of Granular Soil .....	6
2. NUMERICAL METHODS AND PROGRAM CONBAL-P .....	7
2.1 General .....	7
2.2 The Discrete Element Method .....	8
3. NUMERICAL SIMULATIONS .....	11
3.1 Monotonic Loading Simulations .....	11
3.2 Numerical Simulations with Unloading Investigating Initial and Subsequent Yield Loci .....	12
3.3 Micromechanical Observations .....	14
4. CONCLUSION .....	17
REFERENCES .....	18

Accession For	
BTIC GRAB	<input checked="" type="checkbox"/>
BTIC Tab	<input type="checkbox"/>
Unacknowledged	<input type="checkbox"/>
Justification	
By	
Distribution/	
Availability Codes	
Dist	Avail and/or Special
A-1	2.



## ACKNOWLEDGEMENTS

The authors would like to thank the following people and organizations for their valuable assistance in this study:

The Air Force Office of Scientific Research, and especially Lt. Colonel Steven C. Boyce for their continued support throughout this research.

The National Science Foundation, under a grant (MSM 88-17212) from which the computer programs used in this study were developed.

The Cornell National Supercomputer Facility for providing computer time through a grant on the IBM 3090-600E for the computer simulations.

IBM-Kingston, NY, and especially Mrs. Sheu Fang Ma Tzou of IBM who helped two of the authors optimize program CONBAL for parallel processing during a workshop at IBM-Kingston, in December 1989.

Finally, the authors wish to thank Mr. Victor Serrambana and Miss Min Fan undergraduate and graduate students, respectively, at the Department of Civil Engineering at RPI for their help in running some of the simulations.

## ABSTRACT

This report presents the results of a study on the monotonic and cyclic stress-strain behavior of quartz sands and other granular media. Random arrays of elastic rough spheres are used to represent the medium in the numerical simulations which utilize one, two and three sizes of spheres. In all cases the spherical grains are assigned the properties of quartz. Results from a 2D array of 531 grains and from a 3D array of 395 particles are displayed and discussed.

A rigorous representation of granular stress-strain response at small strains and during cyclic loading requires the correct modelling of the force-displacement behavior at the contact between two grains. This was achieved through a numerical solution of the (Hertz-Mindlin) contact problem between two spheres developed by the authors which uses the theory of plasticity and kinematic hardening to describe the phenomenon. The discrete element finite difference method proposed by Cundall and Strack is used to calculate the interactions between particles including geometric rearrangement and formation of new contacts. A periodic space solution is implemented to avoid undesirable boundary effects. All these aspects were incorporated by the authors into program CONBAL-P (CONtact truBAL-Parallel). Because of the large number of contacts, the complex nonlinear character of the contact law, and the explicit nature of the finite difference scheme, a supercomputer is required to run CONBAL-P, which has been optimized for a vector and parallel environment.

The results discussed in the paper focus on identifying the micromechanical phenomena responsible for the motion and distortion of the yield loci of a granular medium in stress space during shear loading that were observed in the laboratory experiments of Volume II. The array is first isotropically compressed and then is sheared at constant mean stress. The shear loading consists of monotonically prestraining the medium to a predetermined level which is followed by unloading and probing in different directions to establish the current size and shape of a yield locus. It has been found that the yield locus distorts in the direction of loading in a way similar to that observed in the laboratory experiments on glass beads. This is in contrast to the current assumption for soils that the yield locus translates without distortion. These results are relevant to the formulation of constitutive relation for granular soil since they indicate that the anisotropic fabric which develops during loading needs to be modelled in order to capture the macroscopic phenomena. The simulations also provide a wealth of statistical information which is used to correlate the macroscopic stress-strain response observed in the laboratory with micromechanical phenomena at the particle contact level.

## 1. INTRODUCTION

### 1.1 General

Over the past 30 years considerable attention has been given to the development of constitutive laws for engineering materials (Hill 1950, Prager 1955, Mroz 1967, Dafalias and Popov 1976, Drucker and Palgen 1981, Yen and Eisenberg 1987). Among other formulations, the existing models are based on the theories of elasticity, hypoelasticity, plasticity and viscoplasticity. Despite the large number of models, there is no consensus yet within the scientific research community on the best approach. However, the models based on the theory of plasticity or viscoplasticity appear to be most promising. Especially critical is the need for a constitutive relation for soils required for analyses of onshore and offshore structures and their foundations, as well as earth structures, subjected to a variety of natural and man-made static and dynamic loading environments. Soil behavior is more complex than that of other materials due to its particulate nature, which makes it pressure-dependent and nonlinear inelastic even at small strains. A large number of models has been proposed for soils based on the theory of plasticity, including those of DiMaggio and Sandler (1971), Baladi and Rohani (1979), Lade (1977), Prevost (1978, 1985), Dafalias and Herrmann (1982). In these models, the total strain is equal to the sum of the elastic and plastic strain increments,  $d\epsilon_{ij} = d\epsilon_{ij}^e + d\epsilon_{ij}^p$  with these increments being rate independent. A variety of associative and non-associative flow rules have been proposed for the plastic strain increment, of the form:

$$d\epsilon_{ij}^p = d\lambda \frac{\partial g}{\partial \sigma_{ij}} \quad (1)$$

where  $\lambda$  is a coefficient of proportionality and  $g(\sigma_{ij})$  is the plastic potential function, which may or may not coincide with the yield function,  $f(\sigma_{ij})$ , at which plastic strains develop. It is typically assumed that these yield surfaces (loci) translate in stress space without distortion (kinematic strain hardening), sometimes increasing or decreasing in size (isotropic strain hardening).

The limitation of these models is that they are phenomenological. They have been typically developed from a manageable mathematical formulation, and they have been calibrated and modified by interpreting macroscopic experimental results, while ignoring the underlying micromechanical phenomena. As a result, the existing plasticity models for soils are in need for constant refinement when needed for cases very different from the one the model was originally developed and calibrated for.

The current situation in metal plasticity is quite different. Although the modelling of the nonlinear behavior of metals started on a similar phenomenological basis, there has been a shift in the last 20 years or so toward formulating the metal response with due consideration of micromechanical principles (Budiansky and Wu 1962, Lin and Ito 1965, 1966). Recently, this has been enhanced by specific experiments and micromechanical (transmission electron microscopy - TEM) measurements (Stout et al. 1985, Helling et al. 1986). The situation is analogous in the modelling of more complex composite materials, where experiments and micromechanical analytical simulations are combined to create the corresponding constitutive law (Dvorak 1987, Dvorak et al. 1988).

A similar effort in soils has begun at RPI by the authors, in which a new constitutive law for granular media is being developed which evolves from several micromechanical studies, including numerical simulations of 2-D and 3-D random arrays of spheres and laboratory experiments on glass beads (Petrakis and Dobry 1989). This paper presents the results of 2 and 3-D simulations of the mechanical behavior of random assemblages of rough, elastic spheres.

### 1.2 Studies on Polycrystalline Aggregates

Starting in the 1950's, researchers have simulated the elastic-plastic, stress-strain behavior of polycrystalline aggregates through analytical, semi-analytical, and numerical micromechanical techniques (Hershey 1954, Budiansky and Wu 1962, Lin and Ito 1965, 1966, Hill 1967, Canova et al. 1985). This micromechanical work has not supported the continuum mechanics hypotheses of either pure kinematic or isotropic hardening behavior, but has predicted a combined translation (kinematic hardening) and distortion of the yield surfaces in the direction of loading.

The micromechanical approach commonly used to analyze the elastic-plastic behavior of polycrystals assumes that they are an assemblage of equal anisotropic monocrystals (single crystals) randomly oriented in space. This results in an isotropic polycrystal if the spatial distribution of the orientations is statistically uniform. A monocrystal has  $n$  sliding planes with each plane having  $m$  sliding directions, and with every sliding direction corresponding to a pair of parallel yield planes in stress space. In the limiting case in which an infinite number of possible crystal orientations is assumed, this infinitely sided polyhedron becomes a curved yield surface.

Plastic strain in the aggregate is caused by sliding of one of the sliding planes occurring in a family of similarly oriented crystals. After sliding has occurred in a number of these families, each surface of the polyhedron mentioned above expands and shifts differently. These sliding directions are all more or less parallel to the direction of the plane of the maximum shear stress acting on the aggregate. As the aggregate is loaded further beyond the elastic range, more crystals and crystal families slide, and increasingly more yield planes pass through the loading point on the yield surface. The yield planes of different orientations intersect at that point on the yield surface and form a corner or vertex.

This vertex is not easily observed during testing. One reason is that the very large number of monocrystal orientations smooths the effect, which appears as a "smooth vertex" or distortion of the yield surface in the direction of loading, rather than a sharp corner. This distortion of the yield surface associated with the vertex reflects the "memory" the material has of prestraining in the direction of loading. The existence of this yield surface distortion in metals has been observed experimentally by a number of researchers in several polycrystalline aggregates, including aluminum alloys, brass and magnesium (Naghdi et al. 1958, Phillips 1968, Kelley and Hosford 1968, Phillips et al. 1970, Shiratori et al. 1976, Helling et al. 1986).

The late Professor Phillips developed a testing procedure to seek and compute the initial and subsequent yield surfaces of aluminum and their motion in stress space (Fig. 1a). This procedure is now widely used in experimental plasticity studies of metals and metal matrix composites (Rousset 1985, Stout et al. 1985, Dvorak 1987, Dvorak et al. 1988). The experiment are typically conducted by applying a combination of tensile and torsional shear stresses to a hollow cylindrical specimen. In these tests, the loading stops and reverses as soon as a point on the yield surface is reached, as defined by a certain deviation from the linear portion of the stress-strain curve. Then the small strain loading (probe) continues until another point on the surface is reached, the load is then reversed, and then increased until enough points have been obtained to accurately define the yield surface (locus). Fig. 1b clearly shows the characteristic distortion of the yield surface in aluminum in the direction of loading. While the yield surface (for a given temperature) in the  $\tau$ - $\sigma$  space is an ellipse, the subsequent yield surfaces have distorted and become pointed in the direction of loading (a), while becoming flatter in the opposite direction (b). As a result, the size of the yield surface shrinks in the direction of loading while staying constant in the other direction.

Laboratory results such as these have made possible the linking of the micromechanical theory with experiments (Stout et al. 1985, Helling et al. 1986), and have led to a new family of

constitutive laws (Phillips and Weng 1975, Eisenberg and Yen 1981, 1984, Yen and Eisenberg 1987) which incorporate the above findings.

### 1.3 Modelling of Granular Soil

The behavior of a sand aggregate is similar to that of a polycrystal, since the individual groups of grains or grain packings within the sand may be considered in first approximation to behave like randomly oriented crystals. The main difference is that the properties of these packings are now pressure dependent. For example, a simple cubic array of equal spheres is a pressure dependent monocrystal having three sliding planes ( $n=3$ ), with each sliding plane containing two sliding directions  $90^\circ$  apart ( $m=2$ ).

As in the case of polycrystalline aggregates, each sliding plane in each of the packings corresponds to a pair of parallel yield planes in stress space. The macroscopic yield surface of the material is the surface bounding the yield polyhedron, the sides of which are formed by the intersection of these yield planes. Plastic strain, defined as *irrecoverable deformation*, is the result of a slide in at least one of these packings. This is directly analogous to the definition of yielding in metals where plastic strain is caused by a slip in one of the slip systems and the term "sliding" in soils is the equivalent of "slip" in metals. However, soils exhibit nonlinear inelastic stress-strain behavior even at small strains which is the result of the force-deformation nonlinearity at the interparticle contacts. Nevertheless, granular soils experience little or no sliding between particle contacts and thus exhibit nondestructive behavior and no dilation up to the so called "threshold shear strain",  $\gamma_t$ , ( $1 \times 10^{-4} < \gamma_t < 2 \times 10^{-4}$ ; Dobry et al. 1982). Therefore, in granular soils, loading below the threshold has some important features in common with elastic loading in metals before the initial yield surface is reached. In soils the loading below  $\gamma_t$  though nondestructive, is inelastic and does include some plastic yielding due to localized slipping within the intergranular contact areas. If this localized slipping effect below  $\gamma_t$  is neglected in first approximation, one possible definition of an initial yield surface in cohesionless soils could be the surface in stress space where  $\gamma_t$  is reached, that is approximately at strains of less than  $2 \times 10^{-4}$ .

## 2. NUMERICAL METHODS AND PROGRAM CONBAL-P

### 2.1 General

The development of a realistic computer program to simulate granular media by random arrays of elastic, rough particles presupposes a number of steps and decisions related to: shapes, sizes, properties and initial spatial distributions of grains, boundary conditions, force-deformation law between two adjacent particles in contact. A numerical scheme needs to be chosen which will allow for individual grain interactions and rearrangements including disappearance of old contacts and formation of new ones. In what follows, some of the solutions provided by the authors in development of their method and associated computer code are discussed.

The problem of the contact of two elastic, elliptical semi-infinite bodies subjected to a normal force was first studied by Hertz (1882). Hertz demonstrated that the normal force-deformation behavior at the contact is nonlinear elastic. Cattaneo (1938), Mindlin (1949) and Mindlin and Deresiewicz (1953) addressed the problem of the contact of two identical elastic, rough spheres subjected to a combination of normal and tangential forces and presented a number of closed form solutions for each of several specific load histories.

Seridi and Dobry (1984) and Dobry et al. (1991) developed a numerical solution for the force-deformation behavior of two elastic, rough spheres in contact under a combination of arbitrarily varying normal and tangential forces, which was then coded as program CONTACT. This model is based on the incremental theory of plasticity, uses an infinite number of yield surfaces (which correspond to an infinite number of contact annuli) and assumes kinematic hardening (Fig. 2). Therefore, its main features are very similar to those of the plasticity stress-strain models for engineering materials described previously.

The numerical solution described previously, implemented in computer program CONTACT was subsequently tested to verify that it reproduces accurately the analytical solutions obtained by Mindlin and Deresiewicz (1953). Once this was done, program CONTACT was made a subroutine which could be used in Finite Element and Discrete Element (Cundall and Strack 1979) simulations.

## 2.2 The Discrete Element Method

Many studies have been performed using particulate models to interpret and model the behavior of cohesionless soils and other granular materials. Most of these investigations have been also included measurements in actual granular soils, as well as in regular or random arrays of spheres (3-D) or disk/rod assemblies (2-D); a number of them have dealt with the load-deformation characteristics at the contact between two elastic bodies possessing friction.

Of special interest are the investigations which have studied the stress-strain behavior of granular arrays considering the elasticity of the particles and the corresponding compliances at the contacts (Duffy and Mindlin 1958, Duffy 1959, Deresiewicz 1958, Walton 1987, Petrakis and Dobry). Serrano and Rodrigues-Ortiz (1973) suggested a method for generating a random configuration of unequal disks or spheres having a prescribed grain size distribution. Cundall and Strack (1979) used a similar approach in conjunction with their distinct element method to successfully simulate the mechanical behavior of arrays of disks and spheres under a variety of loading conditions. In their method, an explicit finite difference formulation is used to determine the static response of the array to applied strains (program TRUBAL) or boundary displacement (program BALL).

Program TRUBAL uses a periodic space in a form of a cube (3-D) or square (2-D), to minimize the effect of boundaries and allow a relatively small number of particles. A uniform strain field is applied to all particles and the corresponding contact forces are calculated from the relative displacements between neighboring spheres. As illustrated by Fig. 3, these contact forces,  $P_i$ , produce in each spheres a resultant unbalanced force  $\Sigma P_i$ , and unbalanced moment  $\Sigma M_i$ , which induce linear and angular accelerations to the particle. These accelerations are used in turn to compute new particle position at the end of a time increment,  $t$ , and new contact forces. The process is repeated until static equilibrium is achieved ( $\Sigma P_i = \Sigma M_i = 0$ ). The method has the advantage of decreasing substantially the required computer memory, as no large stiffness matrices need to be calculated and inverted. However, the execution time is large due to the great number of iterations needed to assure static equilibrium. Initially, TRUBAL was using a linear, non-pressure dependent law to describe the force-deformation behavior at the interparticle contacts; a later version of the program (Zhang and Cundall, 1986) used a linear, pressure-dependent force-deformation relationship.

The existing force-deformation law at the interparticle contacts in program TRUBAL was modified by the rigorous numerical solution to the contact problem (subroutine CONTACT). To

do this, a new array was introduced in TRUBAL which stores the load history at each contact (information on the yield surfaces, elastoplastic moduli, position of apexes, force point etc). The addition of this complex and computationally intensive nonlinear force-deformation law at each interparticle contact increased the computational demands of the program which could no longer be feasible to run on a regular computer. A preliminary study shows that by adding this complex force-deformation law to the program, the computation time increases by a factor of six.

As a result of this, the program was further modified by vectorizing the code to run efficiently on a supercomputer with vector facilities. Recently the code has been parallelized as well, so as to take advantage of a computing environment of six processors. As shown in Fig. 3, since each sphere is treated individually, different contact forces between two different spheres can be calculated simultaneously. To achieve this, the specimen is divided into different zones and the contact forces between different spheres in different zones are calculated at the same times. Calculations in each zone is assigned as a sub task for each of the six processors of the supercomputer used in this study (IBM 3090-600E). For a loading simulation of a very small 3-D specimen (104 spheres), the parallel code in the six processor environment of the Cornell National Supercomputer Facility runs more than twice as fast (in real clock time) as it would run if only one processor was used. The CPU time increases, as expected (see Table 1).

**TABLE 1**

<b>Processing Mode</b>	<b>CPU time</b>	<b>Clock time</b>
Serial (vector)	141 min	210 min
Parallel (6 processors)	140 min	60 min

This performance increase is more dramatic and the computational efficiency improves when larger specimens (more spheres) are used. This new modified program is named CONBAL-P which is essentially a version of TRUBAL incorporating CONTACT and optimized for the supercomputer. Therefore, CONBAL is very similar to original program TRUBAL, except that now the effect of the normal force at the intergranular contacts is included and rigorously modelled. The program CONBAL-P can run in 2-D, in which case the behavior of a monolayer of spheres whose centers lie on the same plane is analyzed, or in 3-D where the behavior of 3-D assemblies of spheres is modelled. Program CONBAL-P has been requiring up to 150MB of primary memory storage to run (depending on the complexity of the loading case and the

complexity of the law modelling the contact behavior) and the computation time for a typical job is 6 CPU hours (vector) on an IBM-3090-600E for a 2-D simulation and 18 CPU hours for a 3-D simulation utilizing the full Mindlin solution without considering particle rotation.

Since the interparticle force-deformation relationships developed by Cattaneo (1938), Mindlin (1949) and Mindlin and Deresiewicz (1953) apply only to spheres of the same size and properties, only random arrays of equal and moderately unequal spheres were developed and studied. Subroutine CONTACT, and thus CONBAL-P can in principle analyze only random arrays of equal spheres; however, the same program, with certain assumptions, can handle in first approximation moderately unequal spheres of the same material. Moreover, the same analytical solutions do not consider rolling of the spheres; consequently rolling is not permitted in the present version of CONBAL-P where the fully nonlinear contact model is utilized. In the case that rotation is not allowed, the coefficient of friction of the material of the spheres has been reduced accordingly (Rowe 1962). A second version of the program allows for particle rotation and a simplified contact model is used, which assumes only one diameter of the contact annulus (sliding - no sliding condition using one yield surface in subroutine CONTACT). This program takes considerably less time to run and has been running on workstations as well.

The accuracy of CONBAL-P has been checked by comparing its results at both small and large strains to a number of available analytical solutions with excellent agreement for both static and cyclic loading under a number of boundary conditions.

The simulations using CONBAL-P can be of great importance to granular media research, because they provide detailed information on any micromechanical variables, such as the distribution of contact angles, the distribution of the mobilized angle (the angle between the shear force and contact normal), the average number of contacts per sphere (coordination number, CN) and their evolution with loading. These simulations can give the same information that Magnetic Resonance Imaging (MRI) would give if applied to a laboratory specimen. The micromechanical information could then be used to interpret the macroscopic behavior.

### 3. NUMERICAL SIMULATIONS

#### 3.1 Monotonic Loading Simulations

As a first step, it was decided to start simulating phenomena in the small strain range ( $10^{-6} < \gamma_i < 10^{-3}$ ), and at a later stage focus on the large strain ( $\gamma_i > 10^{-3}$ ), fully nonlinear inelastic macroscopic behavior. Moreover, it was also decided to compare the results of CONBAL with answers obtained using analytical (Self Consistent, Petrakis and Dobry 1991) and numerical (nonlinear Finite Element, Petrakis and Dobry 1991) procedures developed, as well as with experimental data in the literature and on glass beads presented in Volume II. Results of small strain parametric studies on two 2-D random arrays of spheres, one with 477 equal particles and area porosity (calculated on the plane passing through the sphere centers)  $n = 0.154$  and the other with 531 particles with a ratio of radii  $R_1/R_2 = 1.5$  and area porosity  $n = 0.182$  appear in Petrakis et al. (1989). Parametric studies on a 3-D array of 104 particles with  $R_1/R_2 = 1.5$  and porosity  $n = 0.359$  appear in Ng and Dobry (1990).

The geometrical configuration of the 477 equal particle array subjected to an isotropic confining pressure  $\sigma_o = 91$  KPa is shown in Fig. 4. The configuration of the 531-particle array under  $\sigma_o = 132$  KPa is shown in Fig. 5. In both figures the circles represent the spheres and the rectangles the relative magnitude and direction of the contact force. There are four different rectangle widths, with each one of them corresponding to a range of forces between four equal fractions of the maximum computed contact force. For example, if the maximum contact force is  $F$  KN, the narrowest rectangle stands for the range of forces between 0 and  $F/4$  KN, the next wider rectangle for the range of forces between  $F/4$  and  $F/2$  etc. This notation will be used throughout this report whenever results from the discrete element method are presented.

Figure 6 depicts the geometric configuration of the 3-D 395-particle array under  $\sigma_o = 131$  KPa. In this figure, the difference in color particles identifies their sizes. The 395 sphere 3-D array with the particles assigned the properties of the glass beads used in the experiments of Volume II (Shear Modulus  $G_s = 30$  GPa, Poisson's ratio,  $\nu_s = 0.15$  (instead of 0.21), friction coefficient = 0.32) was first subjected to an isotropic confining pressure  $\sigma_o = 140$  KPa and then the vertical stress,  $\sigma_v = \sigma_{11}$ , was increased while the mean stress was kept constant by unloading the lateral (horizontal) stresses,  $\sigma_{22} = \sigma_{33}$ . This is analogous to a laboratory triaxial compression test on a glass beads where the mean stress is kept constant by reducing the lateral stress (cell pressure)  $\sigma_c = \sigma_2 = \sigma_3$ . The loading was stopped at a octahedral shear strain level  $\gamma_{\alpha\alpha} = \epsilon_1 - \epsilon_3 = 0.3\%$ . The macroscopic stress-strain curve resulting from this simulation appears in Fig. 7a, where the

octahedral shear stress is plotted versus the octahedral shear strain. The volumetric strain appears in Fig. 7b, where it is plotted versus the octahedral shear strain. The same two plots include data from laboratory experiments on glass beads performed as part of this research and presented in Volume II of this report.

### 3.2 Numerical Simulations with Unloading Investigating Initial and Subsequent Yield Loci

The issue investigated is the micromechanical mechanisms controlling the movement and distortion of the yield surface of a granular medium during loading. Analytical considerations and laboratory results presented in Volume II of this report indicate that the yield surface of a granular medium distorts in the direction of loading in a manner analogous to that of polycrystalline aggregates (metals) discussed earlier. In order to investigate the nature these early macroscopic findings and to gain insight into the micromechanical processes occurring at the contact level that shape the macroscopic behavior, a series of 2-D and 3-D numerical simulations were performed using program CONBAL and CONBAL-P, on the 477 and 531 particle 2-D arrays without rotation and on a 395 particle 3-D array with rotation. The stress paths along which these numerical simulations were performed are very similar to those proposed by Phillips and his co-workers and are shown in Fig. 8. Since the numerical simulations in contrast to the laboratory experiments are strain-controlled, all points were first defined in stress space and then their positions were translated to stress space.

The "yield criterion" used was the stress corresponding to a change in the value of octahedral shear strain,  $\gamma_{oct}$ , of 0.024% measured between the point from which the probes start and any point on the yield locus. The procedure has been identical to that used in the laboratory experiments and described in detail in Volume II. The value of  $\gamma_{oct}$  used is not very different from the value for the threshold strain,  $\gamma_t$ , observed in sand,  $0.01 < \gamma_t < 0.02\%$ , discussed earlier in this volume. The numerical media were prestrained to a point in strain space (point 1 in Fig. 8) and then they were unloaded to point 2 which was at a distance from point 1 that was equal to twice the criterion of octahedral strain used ( $\gamma_{oct} = 0.024\%$ ). It was then reloaded by 0.024% from point 2 to point O'. Point O' was used as the reference point for all subsequent small strain loading (probes) to establish the shape of the subsequent yield locus. The rest of the points were obtained by starting from O' and by probing in all directions; this is illustrated in Fig. 8 where the numbers of the points are in the order used to obtain those points. At this small strain level of probing, few inelastic deformations which are the result of geometric changes in the array are expected in the medium after probing from point O'. However, most, if not all, nonlinearity in

the macroscopic stress-strain behavior at this small strain level is expected to be the result of the nonlinear force-deformation behavior at the interparticle contacts.

The 531 array was consolidated to 132 KPa, and then two series of calculations simulating four tests on four initially identical numerical "specimens" were conducted in which the array was prestrained in i) compression to two different strain levels, and ii) in shear to two different strain levels. All four "specimens" were prestrained first to  $\gamma_{\text{oc}} = 0.98\%$  and then to  $\gamma_{\text{oc}} = 2.33\%$ . The mean stress was kept constant to  $\sigma_m = 132$  KPa throughout each simulation.

Figure 9 portrays the results of the 2-D simulations on the 531 particle array in the  $\tau_{12}$ ,  $(\sigma_{11}-\sigma_{22})$  stress space. There are four yield surfaces in this figure, the circular being the initial surface defined by four separate monotonic simulations. The "subsequent" yield surfaces correspond to prestraining to two strain levels,  $\gamma_{\text{oc}} = 0.98\%$  and  $2.33\%$  as marked in two directions (compression,  $\sigma_{11}-\sigma_{22}$ , and shear,  $\tau_{12}$ ). It can be seen that there is a significant change in the shape of the prestrained yield surface: it has shortened in the direction of loading while its dimension in the other direction has not changed. Moreover, this shrinking of the yield surface increases with increasing prestraining. Finally, the surface became flatter in the direction opposite to the direction of loading. While the initial surface has a diameter of 10.6 KPa, the width of the first subsequent locus in the compression direction has decreased to 5.4 KPa and that of the second to 4.8 KPa.

The 477-particle array was consolidated to  $\sigma_m = 91$  KPa and then the same procedure as in the 531 particle array was followed. The array was prestrained to  $\gamma_{\text{oc}} = 0.99\%$  then to  $\gamma_{\text{oc}} = 2.0\%$ . The mean stress was kept constant to  $\sigma_m = 91$  KPa throughout the simulation. The yield surfaces obtained on the 477-equal sphere array are shown in Fig. 10. Again there are five yield surfaces in this figure, the circular being the initial surface defined by the four separate monotonic simulations. Two of the other yield surfaces correspond to the yield loci obtained after the array was prestrained in compression at  $\gamma_{\text{oc}} = 0.99\%$  and  $2.0\%$  respectively, while the other two to those obtained after the array was prestrained in shear at  $\gamma_{\text{oc}} = 0.98\%$  and  $2.3\%$ . All subsequent yield surfaces have shortened in the direction of prestraining, with the width of the surface decreasing as the straining increases. The surfaces have become pointed in the direction of loading and flatter in the opposite direction. The width of the surface in the direction perpendicular to the prestraining direction has not changed. These observations are in good general agreement with the results on the 531 particle array (Fig. 9), but the results are not as smooth or symmetric. This should be attributed to the fact that the 477 equal particle array is not statistically uniform due to crystallization (Fig. 4). This crystallization has lumped the array

into  $N$  constituents, where  $N$  is the number of different packings within the aggregate, and thus has increased the characteristic size of the smallest constituent, from the diameter of the particle to the dimension of the crystalline region. As a result, the array is not completely isotropic under isotropic stress and a much larger number of spheres than 477 is needed in order to have a uniform spatial distribution of the crystallized regions and achieve a statistically isotropic medium.

The 395 3-D array was prestrained to  $\gamma_{oc} = 0.25\%$  and the subsequent yield locus (surface) was obtained by following the same stress paths as in Fig. 8. In this simulation the particles were allowed to rotate and a simplified contact model was used to model the interparticle force deformation behavior. The yield surface obtained appears in Fig. 11 together with the initial locus which was obtained from radial monotonic proportional tests. It can be seen that while the locus has distorted and developed an apex in the direction of loading it has become flatter in the opposite direction. Its width in the direction perpendicular to prestraining has remained approximately the same, indicating that there is a minimal cross-effect.

### 3.3 Micromechanical Observations

The results of these three simulations are in good qualitative agreement with the laboratory data presented in Volume II and are very similar to the yield surfaces obtained in aluminum by Phillips (Fig. 1). As can be seen in Fig. 1, the yield locus (surface) of aluminum distorts in the direction of loading by forming an apex at the loading point and by becoming flatter in the opposite direction. The width of the surface remains the same. While the exact mechanism of the yield locus distortion in metals is not precisely known, it is quite possible that after prestraining, many of the dislocations are pinned at obstacles and are no longer mobile in the forward strain direction (Helling et al. 1986). The resulting high strain gradient elevates the yield point in that direction. When the loading is reversed, these dislocations become mobile again, the yield point is reached easily and the yield locus flattens in that direction. If the loading is continued along a path perpendicular to the prestrain direction, the mobile dislocation density is low and the yield locus cannot be reached easily. Since the prestraining has not mobilized dislocations in that direction, the yield point should be at approximately the same point as the yield point on the stress free material, and in this direction the yield locus should remain at the same point.

The case of granular medium is in a way similar, although large strains in soils are an order of magnitude smaller than in metals. Despite the fact that granular media properties are mean

stress-dependent, this effect can be discounted if the experiments/simulations are performed at constant mean stress. At each of the points in these series of simulations a wealth of statistical information has been accumulated at every point on the surface. Figures 12, 13, 14 and 15 present selected statistical information at the initial state before prestraining and at points 1, 2, and 3 respectively on the 2-D yield locus of Fig. 9. This information includes the distributions of i) contact angle, ii) normalized mobilized angle, iii) coordination number (number of contacts per particle) and iv) the distribution of the contact force. The **normalized mobilized angle** is the angle between the contact force and contact normal normalized by the angle of friction. Therefore, when the normalized mobilized angle is equal to 1, particles are sliding, and if it is equal to 0 contacts are subjected only to a normal force. The difference in signs indicates a different force direction.

As can be seen by the distribution of contact angle in Figs. 12, 13 and 14 there is a clear geometric texture (fabric anisotropy) developing in the direction of prestrain compared to the initial state of the material (Fig. 12). The fabric at this point is controlling the subsequent "yield" behavior of the material, since the strain probes from point O' defining the yield locus (surface) use a strain low enough ( $\gamma_{\text{on}} = 0.02\%$ ) that cannot cause significant geometric changes to the fabric of points on the locus. Consequently, the distribution of the contact angle is very similar for all points on the yield surface (Figs. 13, 14, 15).

The distribution of the normalized mobilized angle is very different from point to point. While the number of spheres sliding does not change significantly (both the coordination number and the number of normalized mobilized planes equal to 1.0 remains the same), what changes dramatically is the distribution of both the mobilized angle and contact force that controls the contacts that will be sliding. For example, when the sample was loaded in compression, contacts were created in the direction of the major applied principal stress while they were lost in the other directions. The Distribution of the mobilized angle and contact force changed accordingly. Consequently, when point 1 was reached and an anisotropic fabric has been created. Once the loading is reversed and the force redistribution takes place, it is easier for the sample to yield in the direction opposite to the loading, due to the texturing which has occurred in the direction of loading. This can be observed through the geometry of the numerical sample at both points (Figs 16 and 17).

The distributions of the **normalized mobilized angle** at points 1 and 2 are very similar to being the mirror image of the other. This suggests that the forces at the particle contacts have changed sign or reversed direction. Moreover, the fact that the specimen geometry has not changed

significantly between these two points, indicates that there are no (or very few) spheres that slid between points 1 and 2. Therefore, there is **slipping** (or rubbing), but not sliding, at the interparticle contacts along the same "paths" that sliding occurred during loading to point 1. Since there are no pinned sliding systems, there are no deformation gradients and the yield locus flattens.

When the sample is loaded by a small strain shear probe, the mobilized angle distribution is analogous to that of the sample before prestraining. This, coupled with the fact that this direction of loading is orthogonal to the prestraining direction no sliding systems have been activated in this direction, results in a yield point similar to that of the original sample. Consequently, the size of the surface does not change perpendicular to the direction of prestraining.

The same is true for the 477 equal particle array as can be seen from the analysis of the geometrical and statistical information presented in Figs. 16-20 for points 1, 2, and 3 on the yield locus of Fig. 9.

The nonlinear distinct element method has been very useful in predicting, as well as interpreting aspects of the behavior of granular medium which could not be determined otherwise. They could not be determined by a distinct element procedure using a linear, non-pressure dependent force deformation law at the interparticle contacts, since this program would be unable to capture the redistribution of contact forces which occur during loading. Nor could these simulations be performed without a supercomputer, since the calculation-demanding relaxation scheme used in the distinct element method, burdened by a nonlinear plasticity program at every contact, could not be solved on a regular computer. As an indication of the complexity of the computations, the CPU time needed to construct Fig. 8 or Fig. 9 was approximately 30 CPU-hours on the IBM 3090-600E. Therefore, as previously hypothesized by the authors, the nonlinear behavior of the granular medium is a result of the particulate nature of the medium and can not be interpreted or reproduced analytically unless this particulate nature is fully modelled and taken into account.

#### 4. CONCLUSION

Nonlinear discrete element simulations have been used to provide an insight on the nonlinear modelling of granular soil. These simulations were based on an incremental solution to the nonlinear problem of two spheres in contact (program CONTACT), incorporated into discrete element TRUBAL which was further optimized for vector and parallel processing on the IBM 3090 supercomputer. It has been found that this approach not only interprets successfully the nonlinear behavior of soil, but also provides a wealth of information on the fabric changes during loading. The yield surface of a granular medium, needed for defining the constitutive relation of such a medium, distorts by forming an apex in the direction of loading while becoming flatter in the opposite direction. This is contrary to the practice followed in modelling granular media where the yield surface of soils are typically assumed to retain the same shape. The origin of this distortion phenomenon lies in the texturing (or fabric anisotropy) which occurs in the direction of prestraining, as well as in the redistribution of interparticle contact forces in the absence of significant particle movement during the small strain probes needed to define the yield surface. These phenomena cause certain slip systems to be activated which in turn produce the characteristic apex which appears in the yield surface in the loading direction. Therefore, the distribution and magnitude of the contact forces are critical for a good understanding of the macroscopic response of the medium. Accurate modelling of the contact force distribution can be achieved only if the behavior at the contact is fully understood and rigorously modelled.

## REFERENCES

- Baladi, G.Y. and Rohani, B. (1979), "Elastic-plastic Model for Saturated Sand, *Journal of the Geotechnical Engineering Division*, ASCE, Vol. 105, No. GT4, April, pp. 465-480.
- Budiansky, B. and Wu, T. (1962), "Theoretical Predictions of Plastic Strains of Polycrystals," *Proc., 4th U.S. Nat. Congr. Appl. Mech.*, pp 1175-1185.
- Canova, G.R., Kocks, U.F., Tome, C.N., Jonas, J.J. (1985), "The Yield Surface of Textured Polycrystals," *J. Mech. Phys. Solids*, Vol. 33, No. 4, pp. 371-397.
- Cattaneo, C. (1938), "Sul Contatto di Due Corpi Elastici". *Atti Acad. Nazionale dei Lincei*, Serie 6, 27, pp. 342-348, 434-436, 474-478.
- Cundall, P. A. and Strack, O. D. (1979), "A Discrete Numerical Model for Granular Assemblies," *Geotechnique*, 29, No. 1, pp. 47-65.
- Dafalias, Y.F. and Popov, E. (1976), "Plastic Internal Variables Formalism of Cyclic Plasticity," *Inter. Symp. on Soils under Cyclic Plasticity, Journal of Applied Mechanics*, Dec., pp. 645-651.
- Dafalias Y.F., and Hermann, L.R. (1982), "Bounding Surface Formulation of Soil Plasticity," *Intl. Symp. on Soils under Cyclic and Transient Loading*, G. Pande and O.C. Zienkiewicz, eds., Wiley, London, U.K., pp. 253-282.
- Deresciewicz, H. (1958), "Mechanics of Granular Matter," *Advances in Applied Mechanics*, V, pp. 233-306, New York: Academic Press Inc.
- DiMaggio, F.L. and Sandler, I.S. (1971), "Material Model for Granular Soils, *Journal of the Engineering Mechanics Division*, ASCE, Vol. 97, pp. 935-950.
- Dobry, R., Ladd, R., Yokel, F.Y., Chung, R.M., Powell, D. (1982), Prediction of Pore Water Pressure Buildup and Liquefaction of Sands During Earthquakes by the Cyclic Strain Method, Building Science Series 138, National Bureau of Standards.
- Dobry, R., Ng, T., Petrakis, E., Seridi, A. (1991), "An Incremental Elastic-Plastic Model for the Force-displacement Relation at the Contact Between Two Spheres," *Journal of Engineering Mechanics*, ASCE, June.
- Drucker, D.C., and Palgen, L. (1981), "On Stress-Strain Relations Suitable for Cyclic and Other Loading," *J. Appl. Mechanics*, September, pp. 479-485.
- Duffy, J. and Mindlin, R.D. (1957), "Stress-Strain Relations of a Granular Medium," *J. Appl. Mech.*, Trans. ASME, Dec., pp. 585-593.

Duffy, J. (1959), "A Differential Stress-Strain Relation for the Hexagonal Close-Packed Array of Elastic Spheres," *J. Appl. Mech.*, pp. 88-94.

Dvorak, G.J. (1987), "Plasticity of Fibrous Composites," Report to U.S. ARO, Dept. Civil Engineering, Rensselaer Polytechnic Institute, Troy N.Y.

Dvorak, G.J. Bahei-El-Din, Y.A., Macheret, Y., and Liu, C.H. (1988), "An Experimental Study of Elastic-Plastic Behavior of a Fibrous Boron Aluminum Composite," Report to ONR, Dept. Civil Engineering, Rensselaer Polytechnic Institute, Troy, N.Y.

Eisenberg, M.A. and Yen, C.F. (1981), "A Theory of Multiaxial Anisotropic Viscoplasticity," *J. Appl. Mechanics*, Vol. 48, June, pp. 276-284.

Eisenberg, M.A. and Yen, C.F. (1984), "The Anisotropic Deformation of Yield Surfaces," *J. Engineering Materials and Technology*, Vol. 106, Oct., pp. 355-360.

Helling, D.E., Miller, A.K., and Stout, M.G. (1986), "An Experimental Investigation of the Yield Loci of 1100-0 Aluminum, 70:30 Brass and an Overaged 2024 Aluminum Alloy After Various Prestrains," *J. of Engineering Materials and Technology*, Vol. 108, pp. 313-320.

Hershey, A.V. (1954), "The Elasticity of an Isotropic Aggregate of Anisotropic Cubic Crystals," *J. Appl. Mechanics*, Vol. 21, pp. 236.

Hertz, H. (1882), "Uber die Behrungs-fester Elastischer Korper". *J. Reine Angew. Math.*, 92, pp. 156-171.

Hill, R. (1950), The Mathematical Theory of Plasticity, Oxford University Press, London, U.K.

Hill, R. (1967), "The Essential Structure of Constitutive Laws for Metal Composites and Polycrystals," *J. Mech. Phys. Solids*, Vol. 15, pp. 79-95.

Kelley, E.W., and W.F. Hosford (1968), "The Deformation Characteristics of Textured Magnesium," *Transactions of the Metallurgical Society of AIME*, Vol. 242, April, pp. 654-660.

Lade, P.V. (1977), "Elastoplastic Stress-Strain Theory for Cohesionless Soil with Curved Yield Surfaces," *Int. J. Solids Structures*, Vol. 13, pp. 1019-1035.

Lade, P.V. and Duncan, J.M. (1975), "Elastoplastic Stress-Strain Theory for Cohesionless Soil," *Journal of Geotechnical Engineering Division, ASCE*, Vol. 101, No. GT10, pp. 1177-1194.

Lin, T.H. and Ito, M. (1965), "Theoretical Plastic Distortion of Polycrystalline Aggregate under Combined and Reversed Stresses," *J. Mech. Phys. Solids*, Vol. 13, pp. 103-115.

Lin, T.H. and Ito, M. (1966), "Theoretical Plastic Stress-Strain Relationship of a Polycrystal and the Comparison with the Von Mises and the Tresca Plasticity Theories," *Intl. J. Eng. Sci.*, Vol. 4, pp. 543-561.

Mindlin, R.D. (1949), "Compliance of Elastic Bodies in Contact", *Journal of Applied Mechanics*, Sept., pp. 259-268.

Mindlin, R.D. and Deresiewicz, H. (1953), "Elastic Spheres in Contact Under Varying Oblique Forces," *J. Appl. Mech.*, Trans. ASME, Sept., pp. 327-344.

Mroz, Z. (1967), "On the Description of Anisotropic Workhardening," *J. Mech. Phys. Solids*, Vol. 15, pp. 163-175.

Naghdi, P.M., Essenburg, F., and Knoff, W. (1958), "An Experimental Study of the Initial and Subsequent Yield Surfaces in Plasticity," *J. Appl. Mech.*, June, pp. 201-209.

Ng, T.-T. (1989), "Numerical Simulations of Granular Soil under Monotonic and Cyclic Loading: A Particulate Mechanics Approach". Dissertation submitted to the graduate School at Rensselaer Polytechnic Institute as a partial fulfillment of the requirement for the degree of Doctor of Philosophy. Rensselaer Polytechnic Institute, Troy, NY.

Ng, T.-T. and Dobry R. (1991), "A Nonlinear Numerical Model for Soil Mechanics". Submitted for possible publication to the *International Journal for Numerical and Analytical Methods in Geomechanics*.

Petrakis, E. (1987) "Behavior of Anisotropic Sand Under loading With Variable Inclination of Principal Stress". First Panhellenic Conference in Soil Mechanics, Athens, Greece, February.

Petrakis, E. and Dobry R. (1989) "Micromechanical Behavior and Modelling of Granular Soil". Report to the US AFOSR, Department of Civil Engineering, Rensselaer Polytechnic Institute, Troy, NY

Petrakis, E. and Dobry R. (1991), "Small Strain Elastic Constants of Precycled Sands by the Self-Consistent Method." Submitted for possible publication to *Geotechnique*.

Petrakis, E., Dobry R. and Stokoe, K.H. (1991), "A 2-D Model for the Small Strain Response of Granular Soil." Submitted for possible publication to *Geotechnique*.

Petrakis, E., Dobry R., and Ng, T.T. (1989), "Small Strain response of Random Arrays of Elastic Spheres Using a Nonlinear Distinct Element Procedure," International Symposium on Wave Propagation in Granular Media, ASME Annual Meeting, San Francisco, December

Phillips, A. (1968), "Yield Surfaces of Pure Aluminum at Elevated Temperatures," IUTAM-Symposium on Thermoelasticity, pp. 241-258.

Phillips, A., Liu, C.S., and Justusson, J.W. (1970), "An Experimental Investigation of Yield Surfaces at Elevated Temperatures," *Acta Mechanica*, Vol. 14, pp. 119-146.

Phillips, A. and Tang, J.L. (1972), "The Effect of Loading Path on the Yield Surface at Elevated Temperatures," *Int. J. Solids and Structures*, Vol. 8, pp. 463-474.

Phillips, A., Tang, J.L., and Ricciutti, M. (1974), "Some New Observations on Yield Surfaces", *Acta Mechanica*, **20**, pp. 23-29.

Phillips, A. and Weng, G.J. (1975), "An Analytical Study of an Experimentally Verified Hardening Law," *J. Appl. Mech.*, June, pp. 375-378.

Prager, N. (1955), "The Theory of Plasticity: A Survey of Recent Achievement, Proceedings Inst. Mech. Eng., Vol. 169, pp. 41-57, London, U.K.

Prevost, J.H. (1978), "Plasticity Theory for Soil Stress-Strain Behavior," *Journal of the Engineering Mechanics Division*, ASCE, Vol. **104**, No. EM5, pp. 1177-1194.

Prevost, J.H. (1985), "A Simple Plasticity Theory for Frictional Cohesionless Soils, *Soil Dynamics and Earthquake Engineering*, Vol. **4**, No. 1, pp. 9-17.

Rousset, M. (1985), "Surface Seuil de Plasticite: Determination Automatique et Modelisation", These de Docteur Ingenieur, Laboratoire de Mecanique et Technologie, Universite Pierre et Marie Currie, Paris-6, Cachan, France.

Rowe, P.W. (1962), "The Stress-Dilatancy Relation for Static Equilibrium of an Assembly of Particles in Contact," *Proc. Royal Soc.*, **A269**, pp. 500-527.

Seridi, A. and Dobry, R. (1984), "An Incremental Elastic-Plastic Model for the Force-Displacement Relation at the Contact Between Two Spheres," Research Report, Dept. of Civil Engineering, Rensselaer Polytechnic Institute, Troy, N.Y.

Serrano, A.A. and Rodriguez-Ortiz, J.M. (1973), "A Contribution to the Mechanics of Heterogeneous Media", Symp. on Plasticity and Soil Mechanics, Cambridge England.

Shiratori, E., Ikegami, K. Yoshida, Kaneko, K. and Koike, S. (1976), "The Subsequent Yield Surfaces after Preloading under Combined Axial Load and Torsion", *Bulletin of the ISME*, Vol. **19**, No. 134, August, pp. 877-883.

Strack, O.D.L. and Cundall, P.A. (1984), "Fundamental Studies of Fabric in Granular Materials". Interim report to NSF CEE 8310729, Department of Civil and Mineral Engineering, University of Minnesota, Minneapolis, MN.

Stout, M.G., Martin, P.L., Helling, D.E., and Canova, G.R. (1985), "Multiaxial Yield Behavior of 1100 Aluminum Following Various Magnitudes of Prestrain," *Int. J. of Plasticity*, Vol. **1**, pp. 163-174.

Walton, K. (1978), "The Oblique Compression of Two Elastic Spheres". *Journal of the Mechanics and Physics of Solids*, Vol. **35**, pp. 213-226.

White, J.E. (1965) Seismic Waves, McGraw-Hill, New York.

Yen, C.F. and Eisenberg, M.A. (1987), "The Role of a Loading Surface in Viscoplasticity Theory," *Acta Mechanica*, **69**, pp. 77-96.

Zhang, Y. and Cundall, P.A. 1986, "Numerical Simulations of Slow Deformations". Proceedings, Tenth US National Congress of Applied Mechanics, Univ. Texas, Austin, TX.

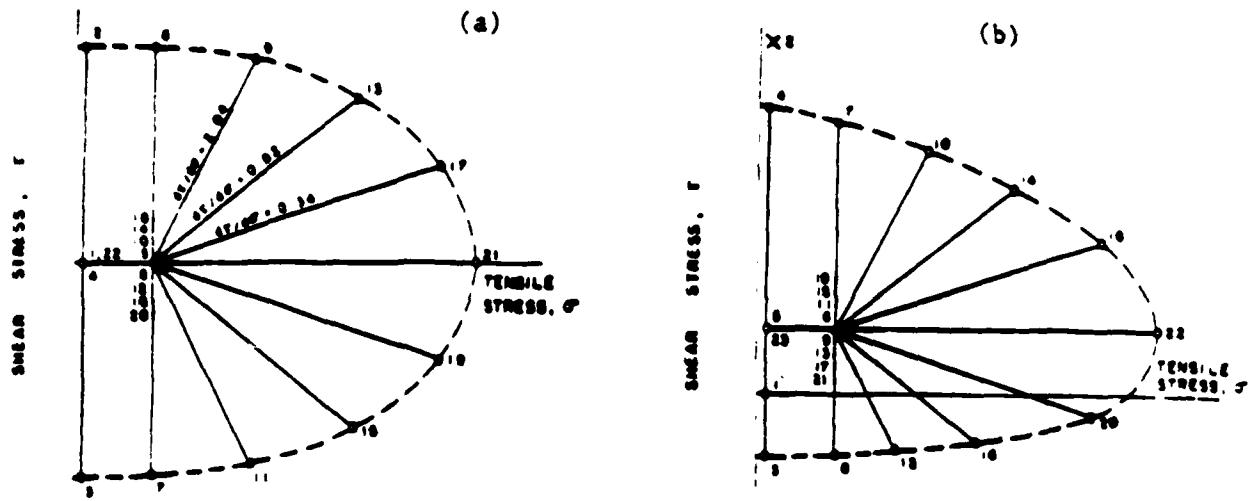


Fig. 1a. Loading paths for (a) initial, and (b) subsequent yield surfaces (Phillips 1968)

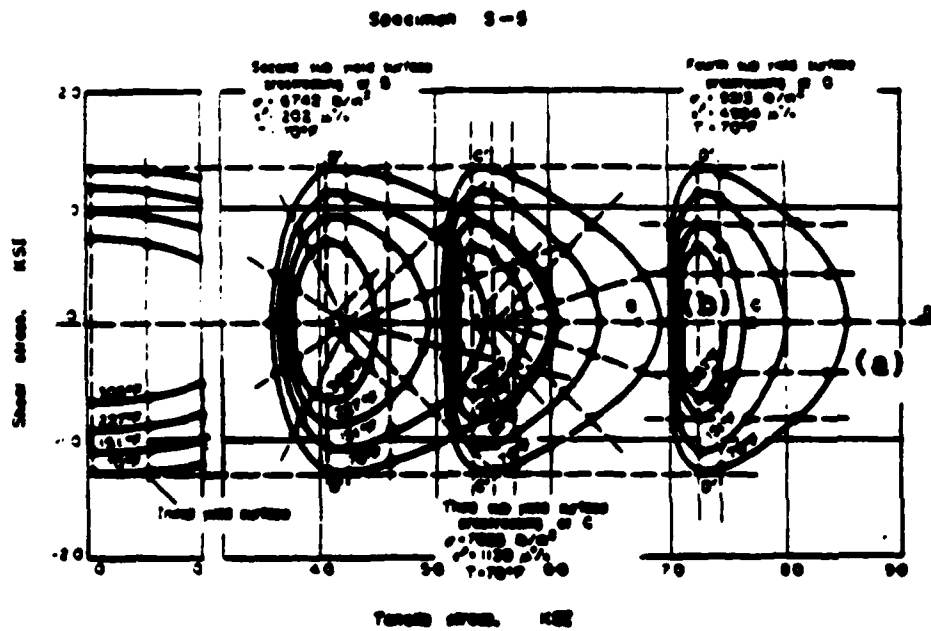


Fig. 1b. Experimentally obtained initial and subsequent yield surfaces for aluminum at different temperatures.

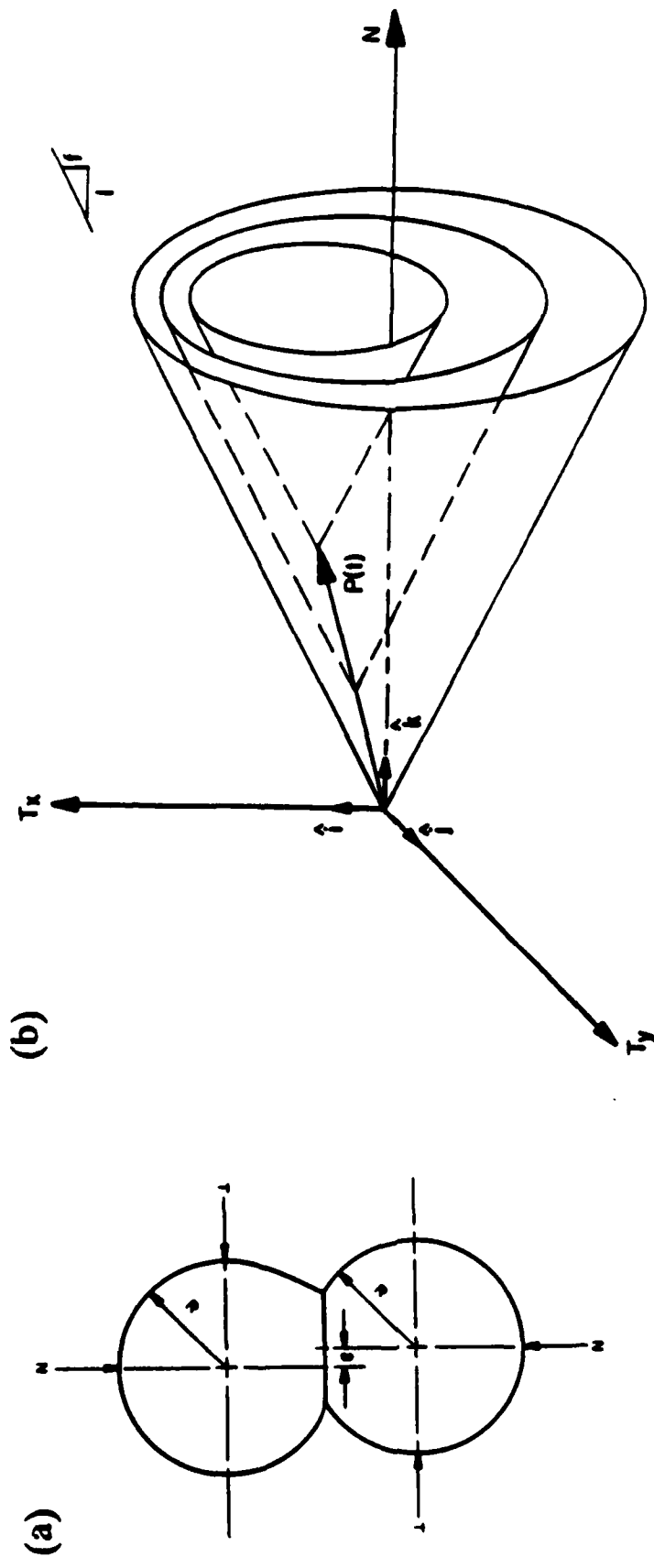
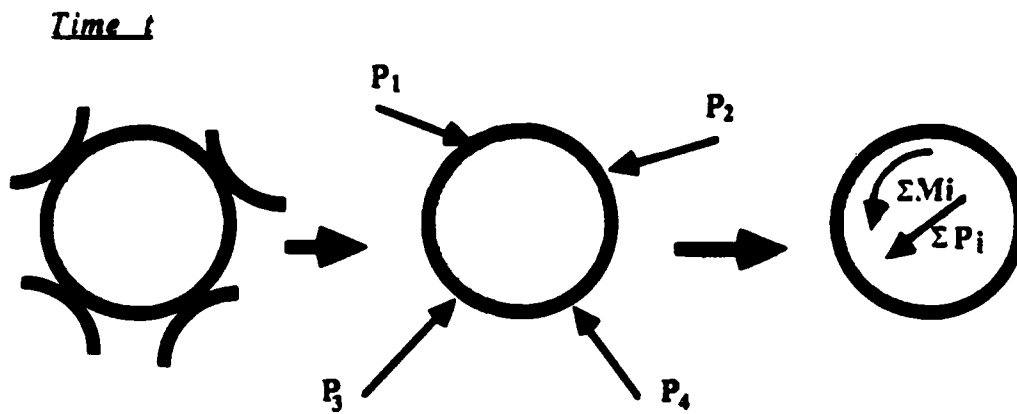


Figure 2. (a) Elastic Spheres Under Normal and Tangential Loads, (b) Contact Force Space and Conical Yield Surfaces: Elastic-Plastic Incremental Solution of the Hertz-Mindlin Problem (Seridi and Dobry 1984).



$\Sigma Pi$  produces acceleration of particle  
 $\Sigma Mi$  produces angular acceleration (spin) of particle

Acceleration and Spin Computed as if Neighboring Particles did not exist. Time step is assumed to be small such that accelerations and velocities are constant in this small time.

Time t +  $\Delta t$

- Particle occupies new position due to acceleration
- New  $P_i$ 's,  $M_i$ 's are computed for new positions
- $\Sigma Pi$ ,  $\Sigma Mi$  and process is repeated.

Figure 3. Main Features of the Discrete Element Method

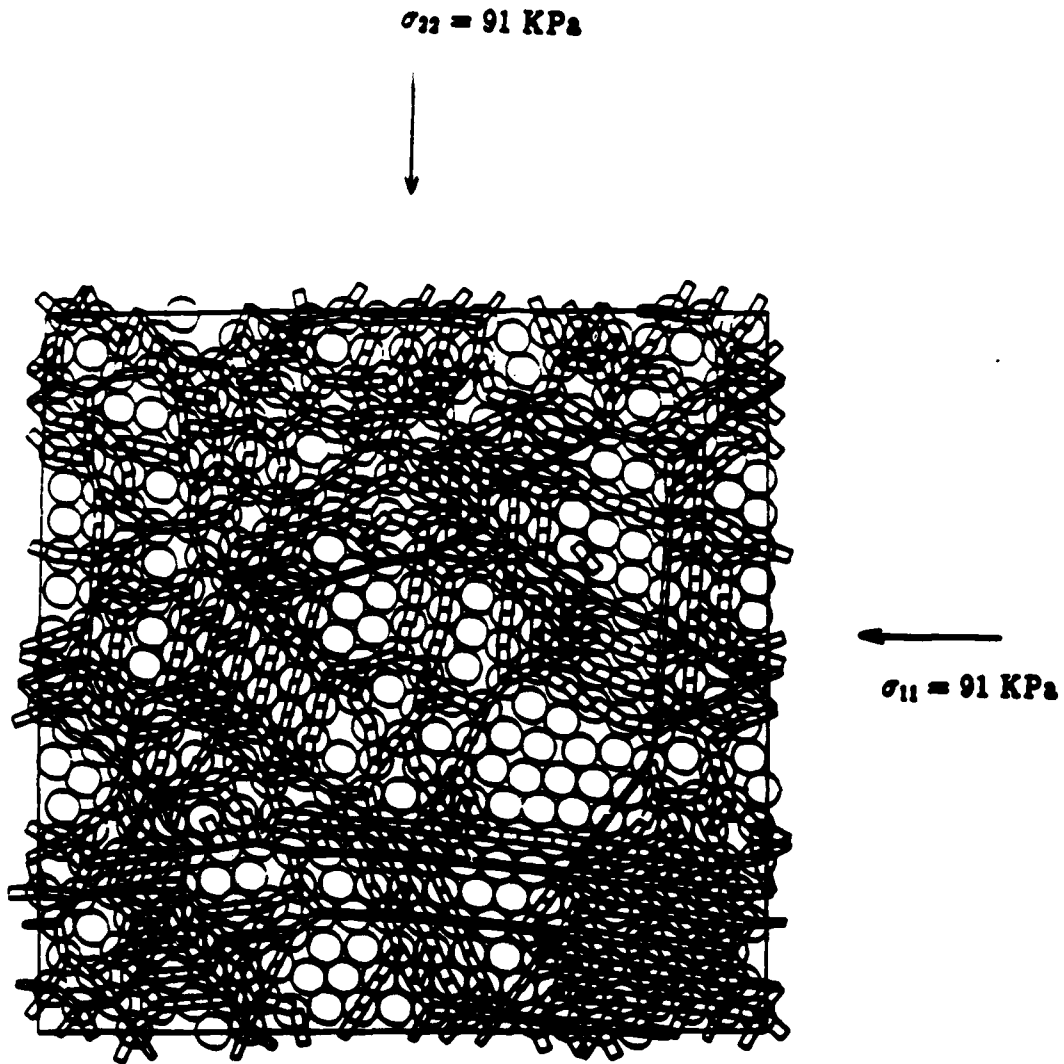


**Fig. 4.** 2-D random array of 477 equal, elastic, rough spheres assigned the properties of quartz, subjected to isotropic compression. This figure represents the "element" of the periodic space.

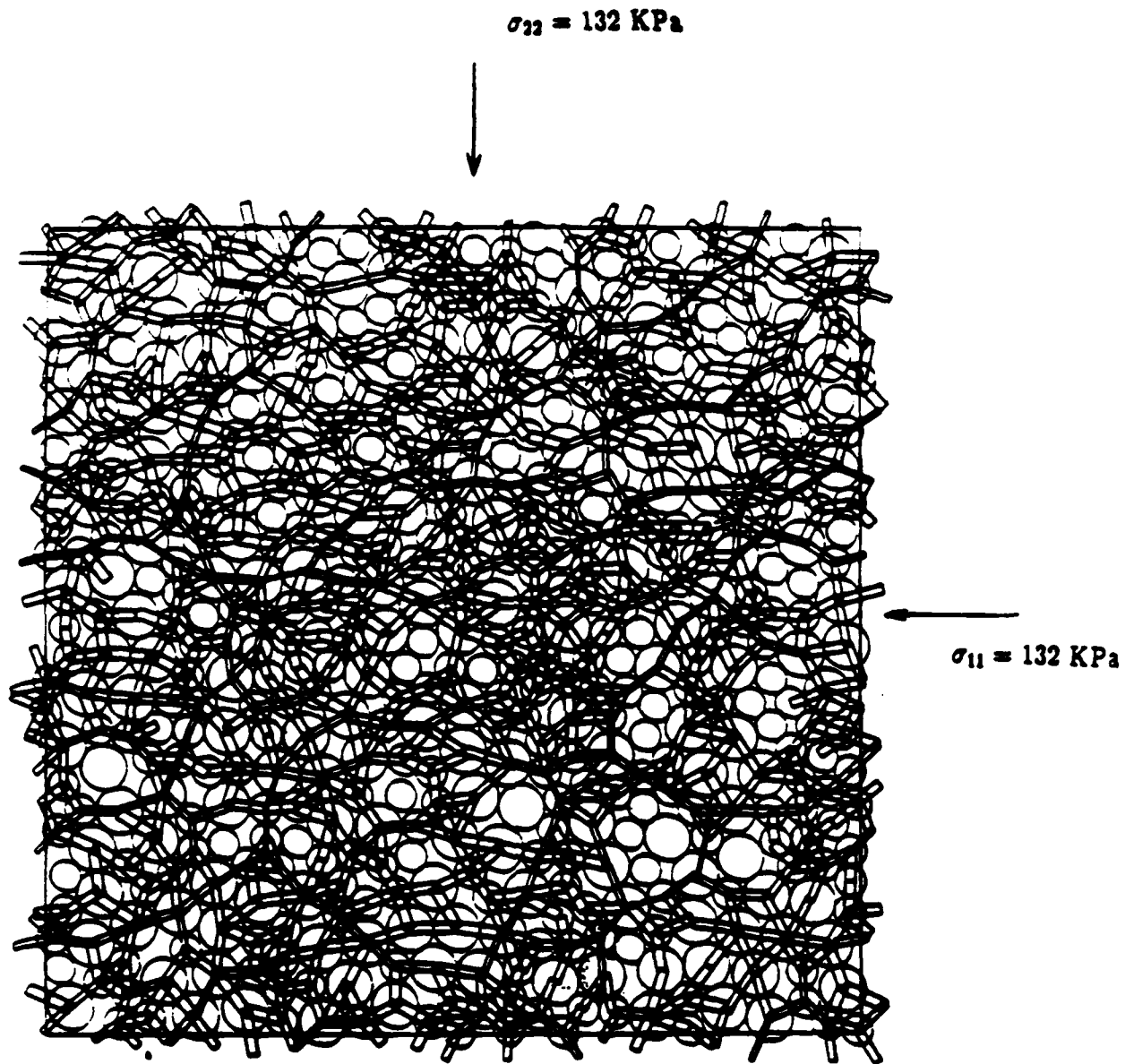


Fig. 5. 2-D random array of 531 elastic, rough spheres with two radii ( $R_1 / R_2 = 1.5$ ) assigned the properties of quartz, subjected to isotropic compression. This figure represents the "element" of the periodic space.

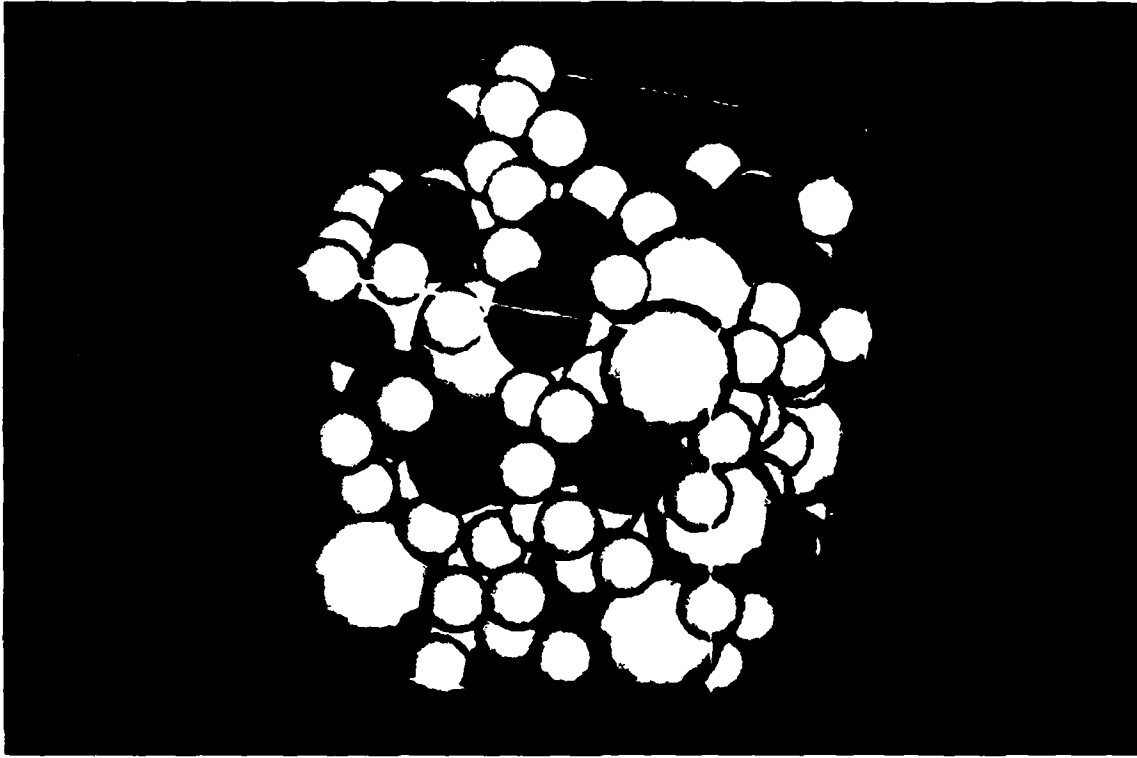


Fig. 6. Initial configuration of the 3-D random array of 365 elastic, rough spheres with three radii.

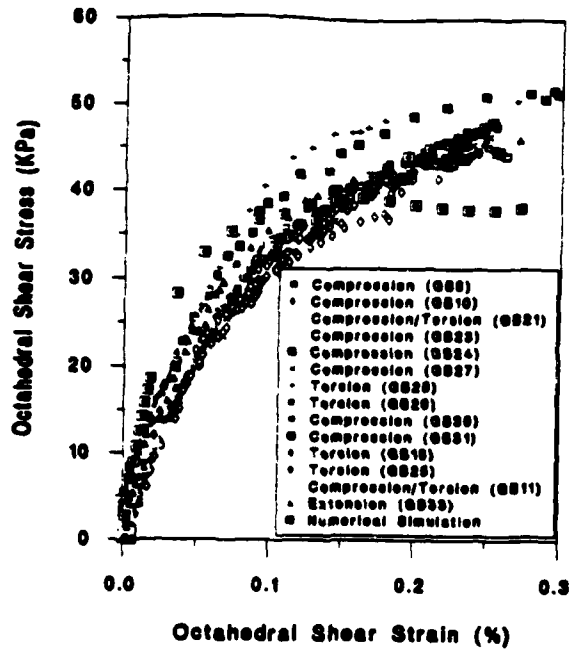


Fig. 7a. Comparison between the octahedral stress - strain curves obtained by the 3-D numerical simulation and laboratory experiments.

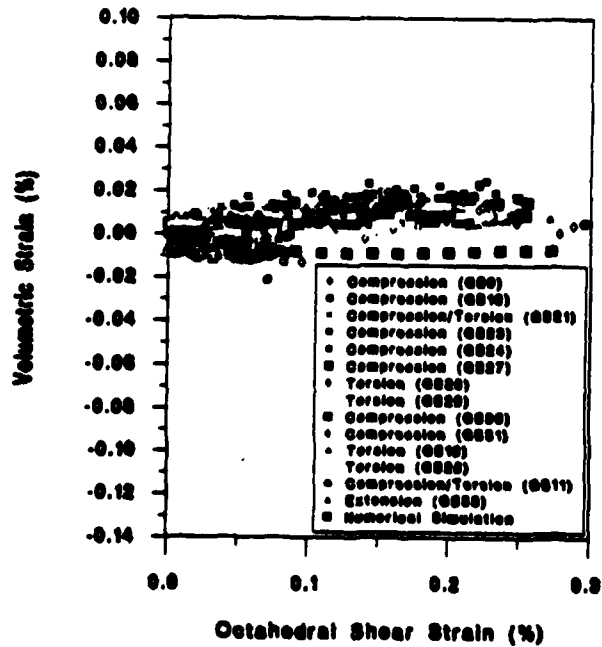


Fig. 7b. Comparison between the volumetric strain - octahedral shear strain curves obtained by the 3-D numerical simulation and laboratory experiments.

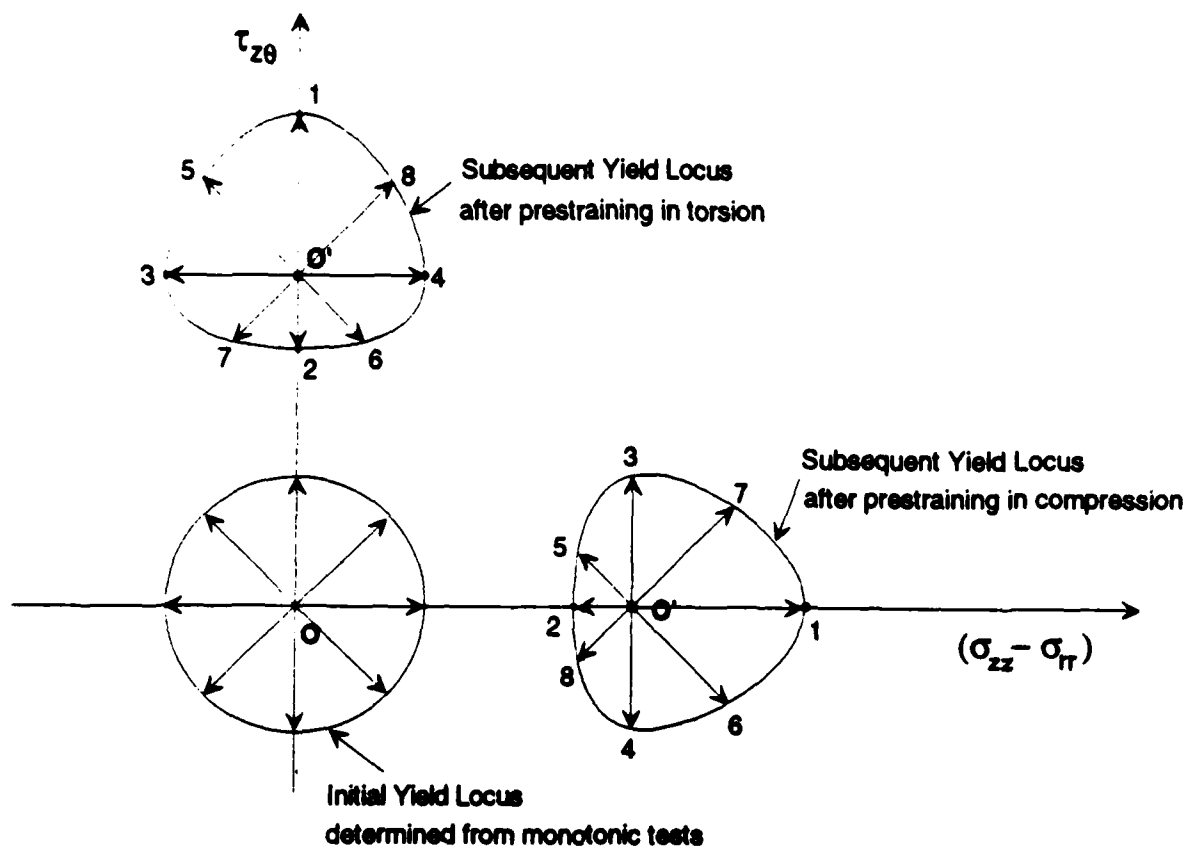


Fig. 8. Stress paths in stress space used in determining the initial and subsequent yield loci in the numerical simulations.

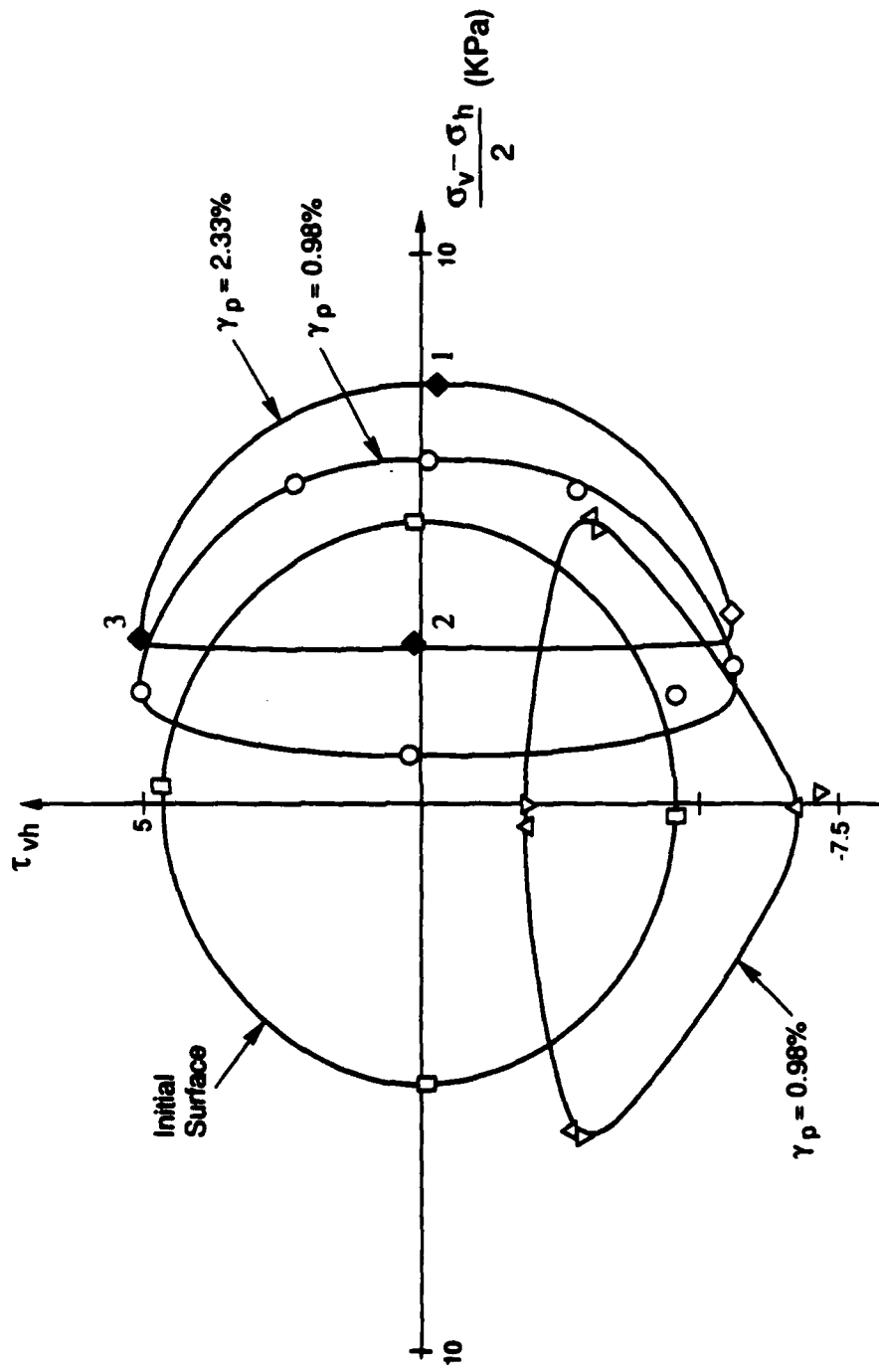


Fig. 9. Initial and subsequent yield loci obtained for the S31 particle 2-D array. Prestraining as indicated.

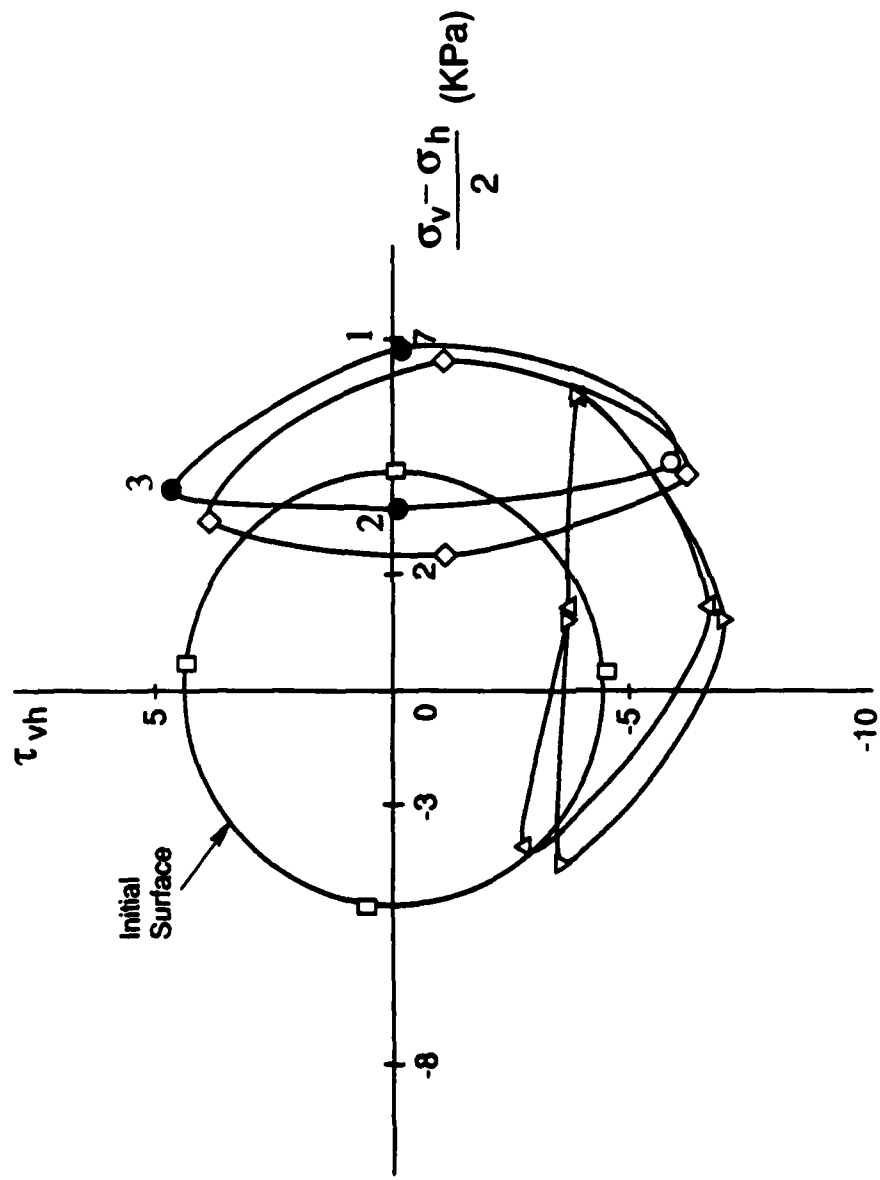


Fig. 10. Initial and subsequent yield loci obtained for the 477 particle 2-D array.

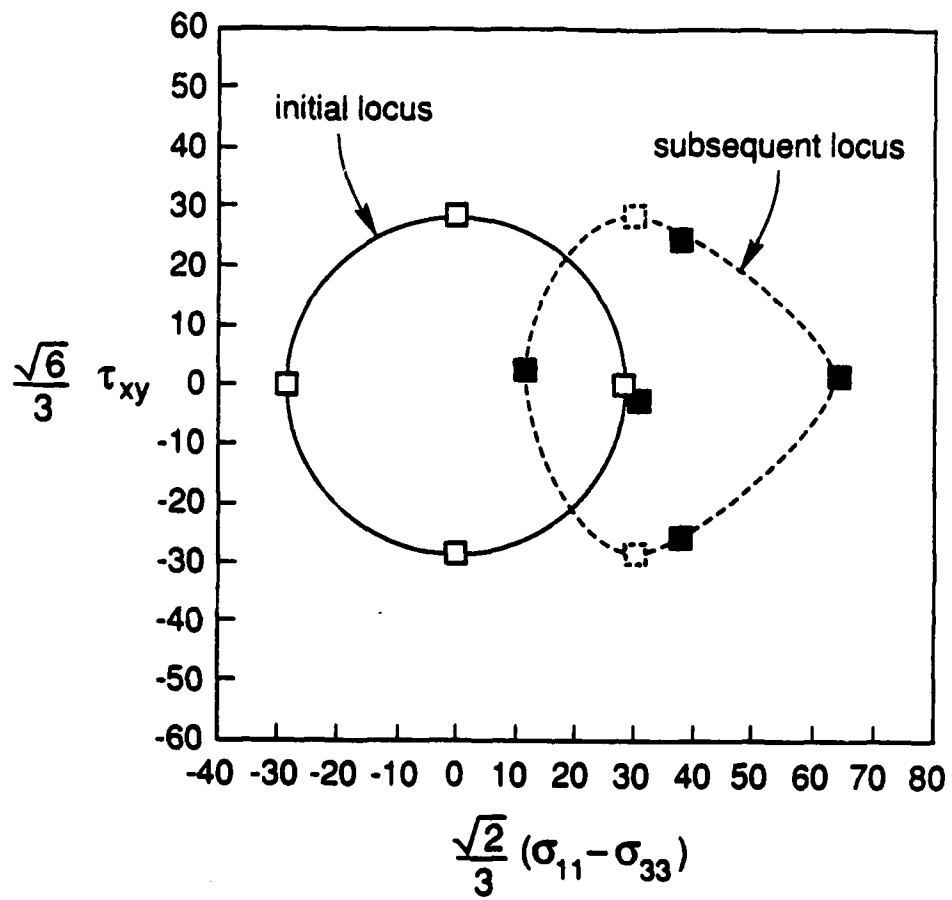
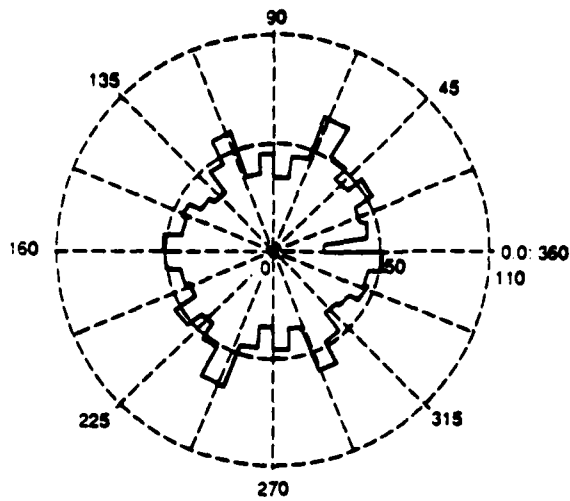
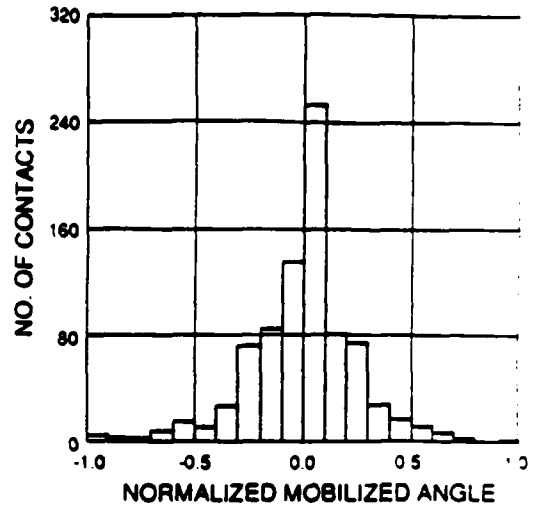


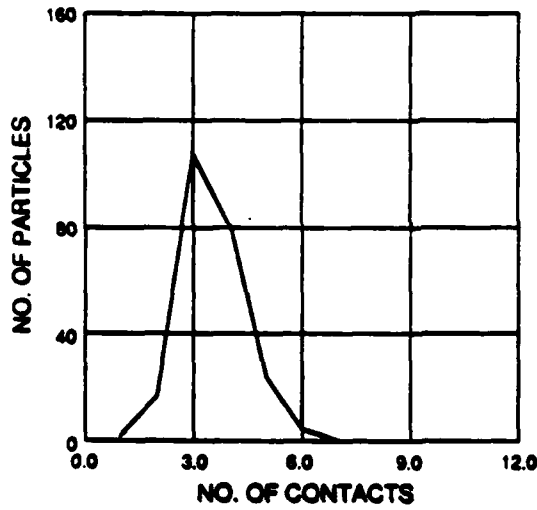
Fig. 11. Initial and subsequent yield loci obtained for the 365 particle 3-D array. Prestraining as indicated.



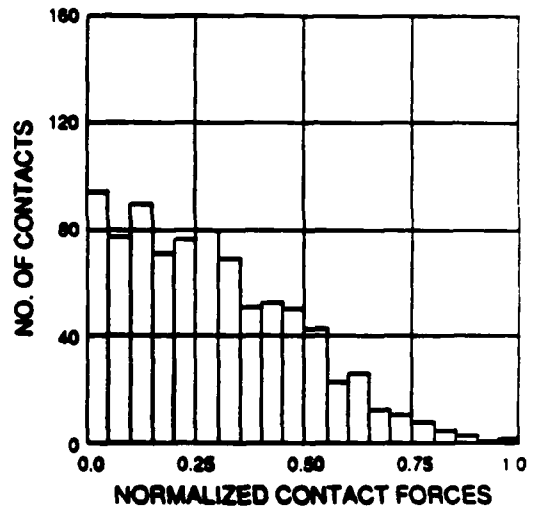
FREQUENCY DISTRIBUTION OF CONTACT ANGLE



FREQUENCY DISTRIBUTION OF MOBILIZED ANGLE

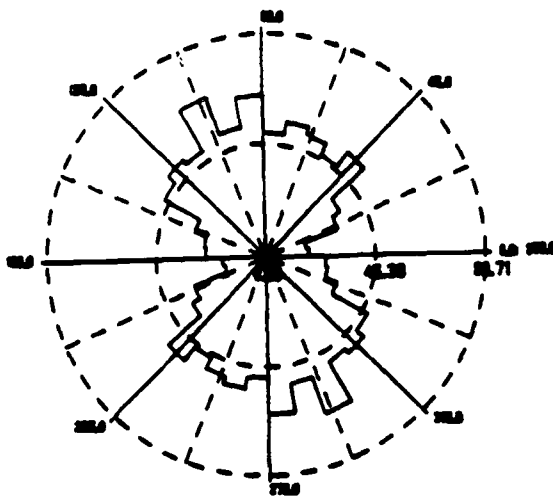


FREQUENCY DISTRIBUTION OF CONTACT PER PARTICLE

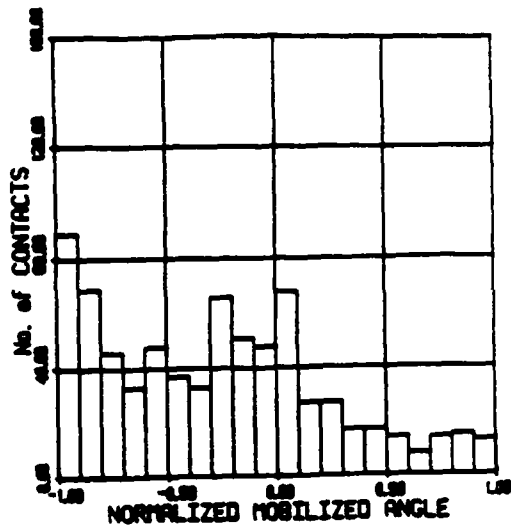


FREQUENCY DISTRIBUTION OF CONTACT FORCE

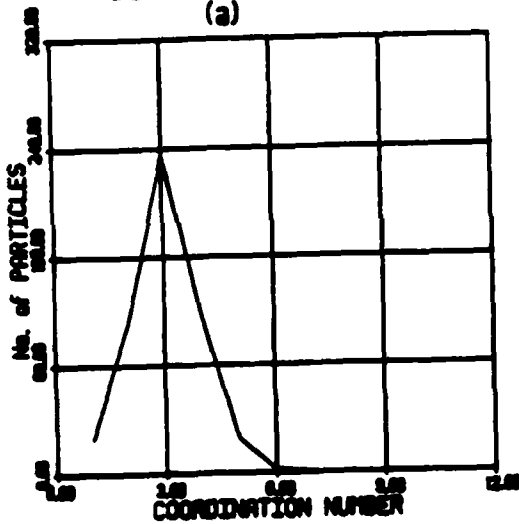
Fig. 12. Statistical Information regarding the state of the 531 particle array of Fig. 5 under isotropic pressure,  $\sigma_m = 132$  KPa.



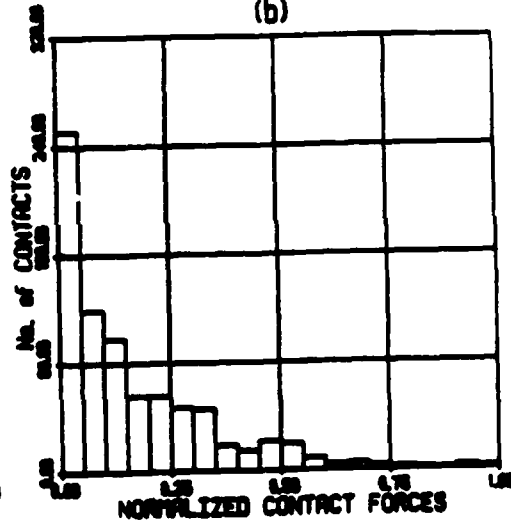
DISTRIBUTION OF CONTACT ANGLE  
(a)



DISTRIBUTION OF MOBILIZED ANGLE  
(b)

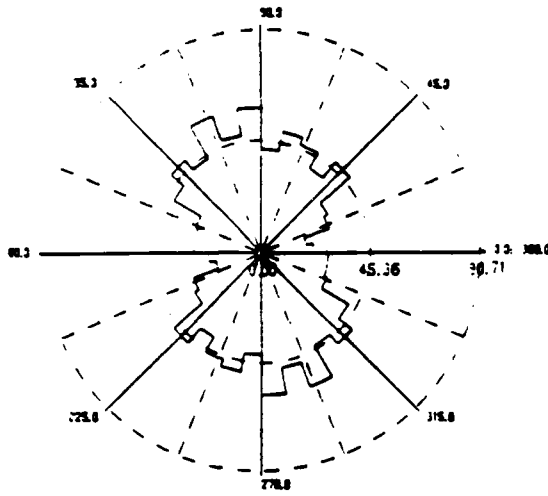


DISTRIBUTION OF CONTACTS PER PARTICLE  
(c)

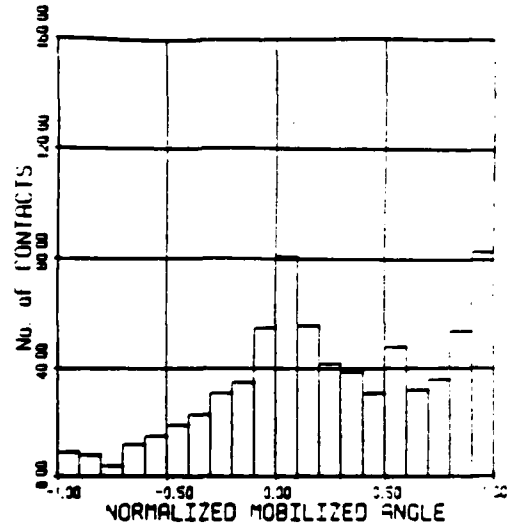


DISTRIBUTION OF CONTACT FORCE  
(d)

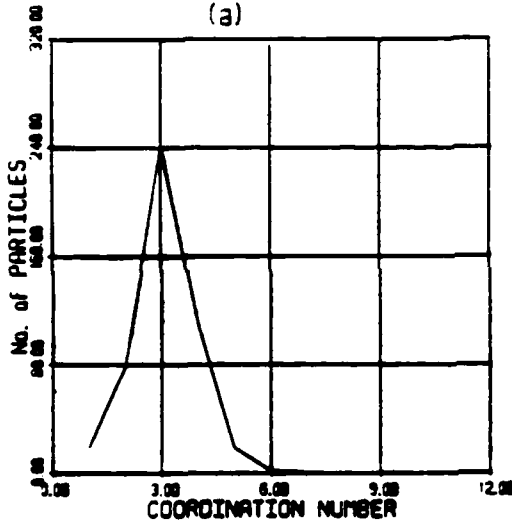
Fig. 13. Statistical Information regarding the state of the 531 particle array of Fig. 5 at point 1 on the yield surface of Fig. 9.



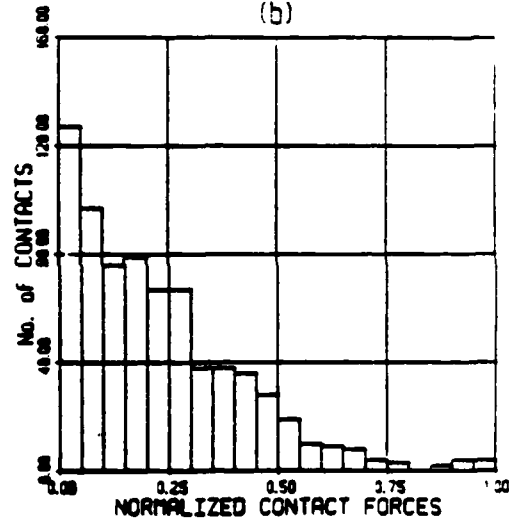
DISTRIBUTION OF CONTACT ANGLE  
(a)



DISTRIBUTION OF MOBILIZED ANGLE  
(b)



DISTRIBUTION OF CONTACTS PER PARTICLE  
(c)



DISTRIBUTION OF CONTACT FORCE  
(d)

Fig. 14. Statistical Information regarding the state of the 531 particle array of Fig. 5 at point 2 on the yield surface of Fig. 9.

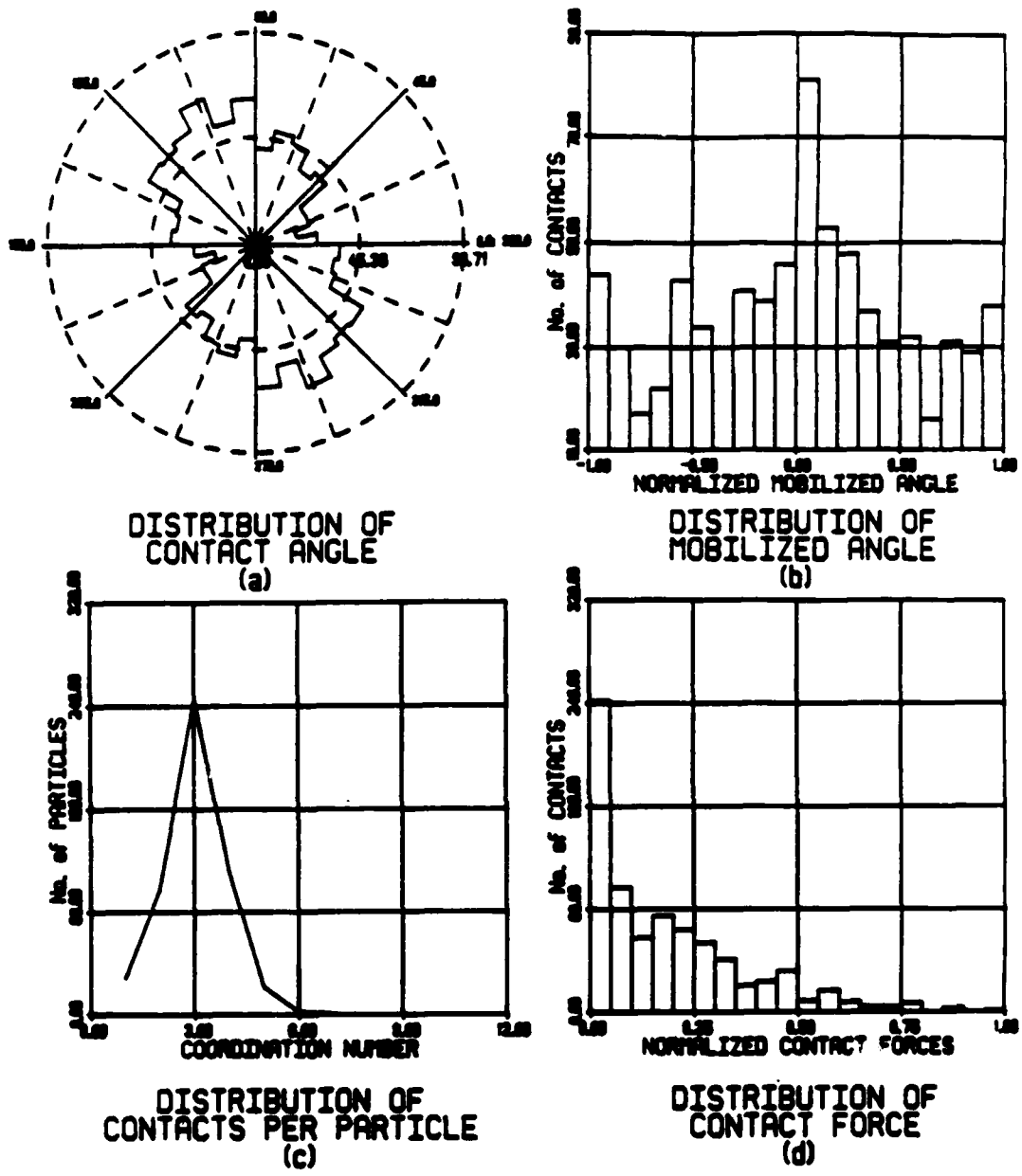
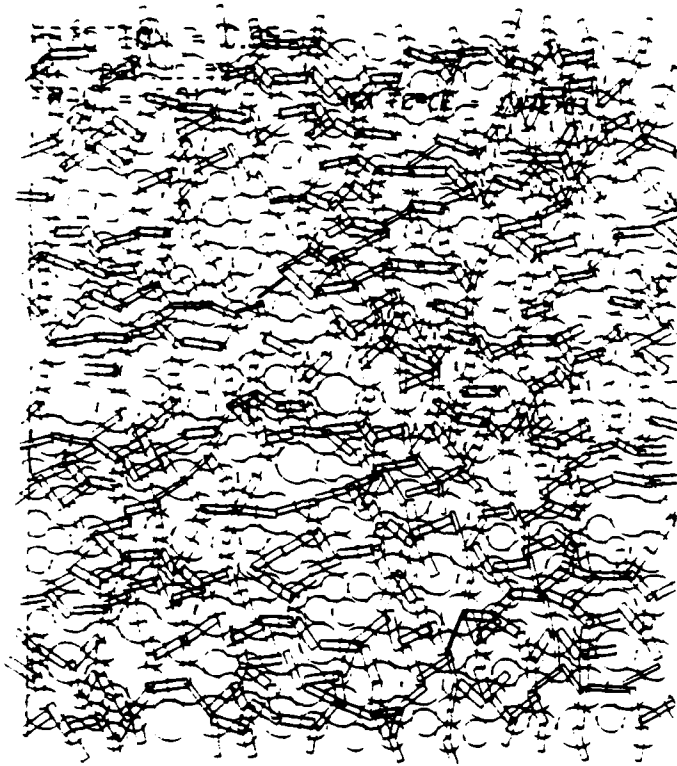
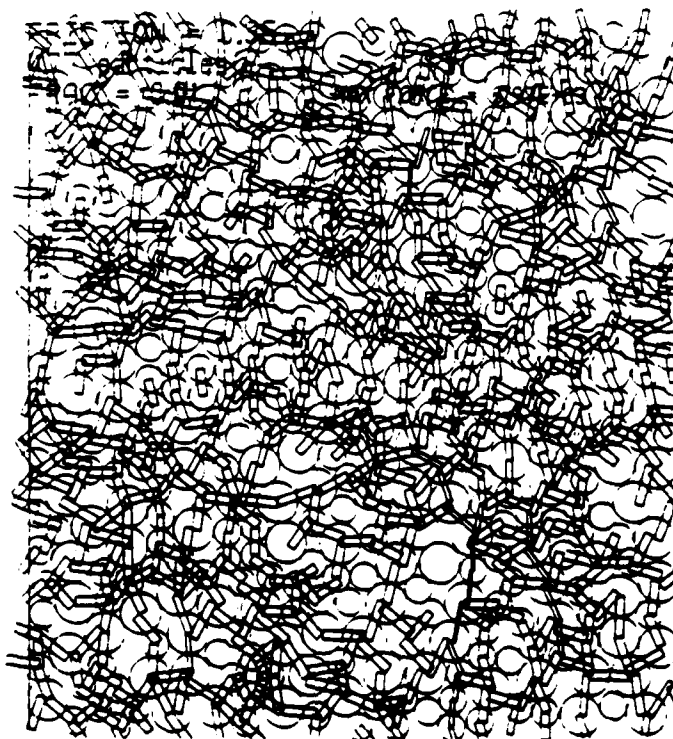


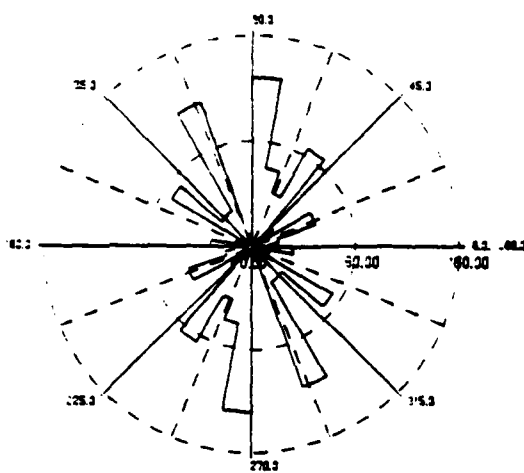
Fig. 15. Statistical Information regarding the state of the 531 particle array of Fig. 5 at point 3 on the yield surface of Fig. 9.



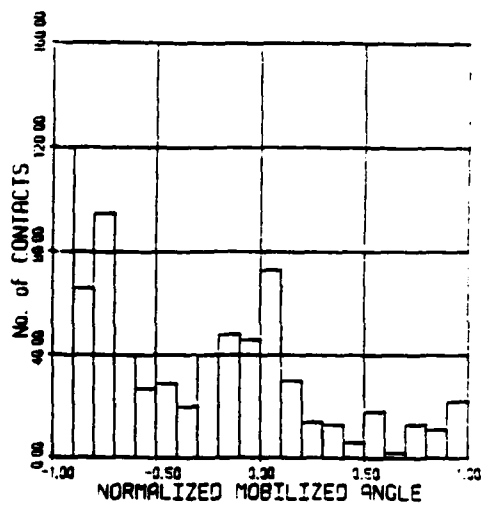
**Fig. 16.** Geometry and contact force distribution of the 531 particle array of Fig. 5 at point 1 on the yield surface of Fig. 9.



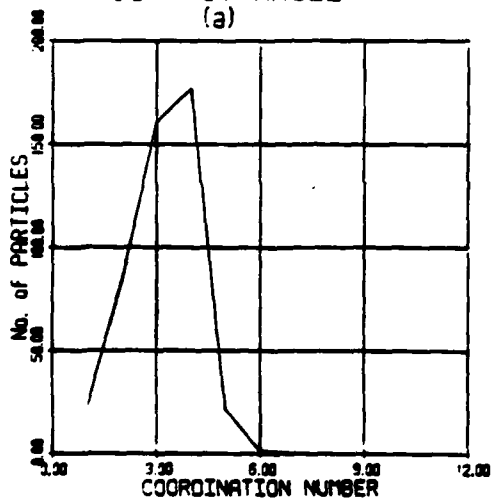
**Fig. 17.** Geometry and contact force distribution of the 531 particle array of Fig. 5 at point 2 on the yield surface of Fig. 9.



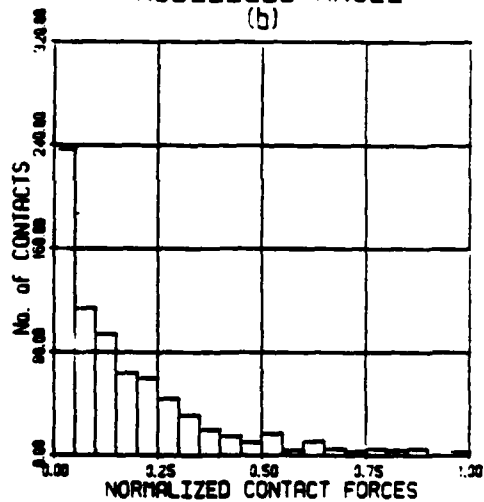
DISTRIBUTION OF CONTACT ANGLE  
(a)



DISTRIBUTION OF MOBILIZED ANGLE  
(b)



DISTRIBUTION OF CONTACTS PER PARTICLE  
(c)



DISTRIBUTION OF CONTACT FORCE  
(d)

Fig. 18. Statistical Information regarding the state of the 477 particle array of Fig. 4 at point 1 on the yield surface of Fig. 10.

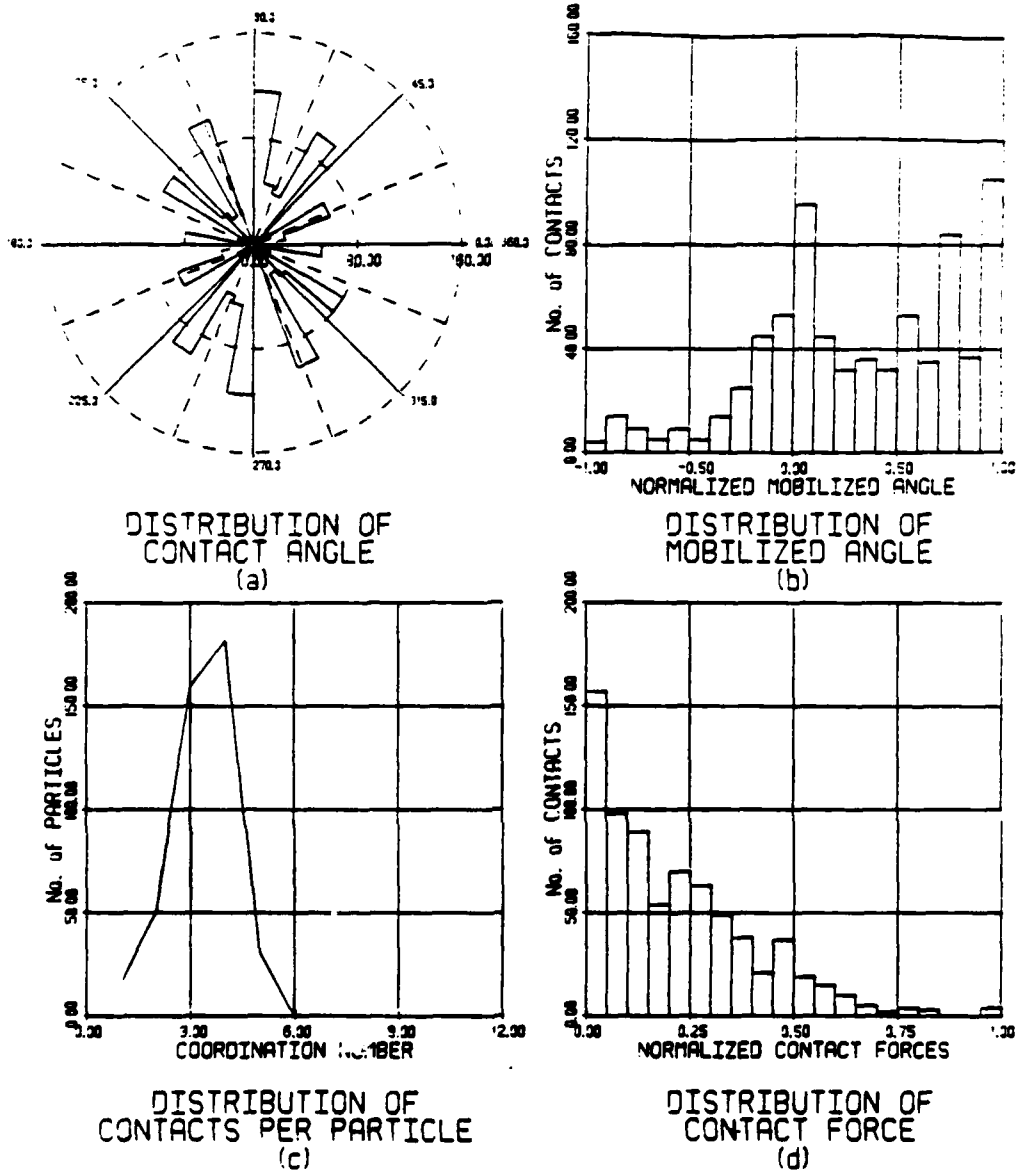


Fig. 19. Statistical Information regarding the state of the 477 particle array of Fig. 4 at point 2 on the yield surface of Fig. 10.

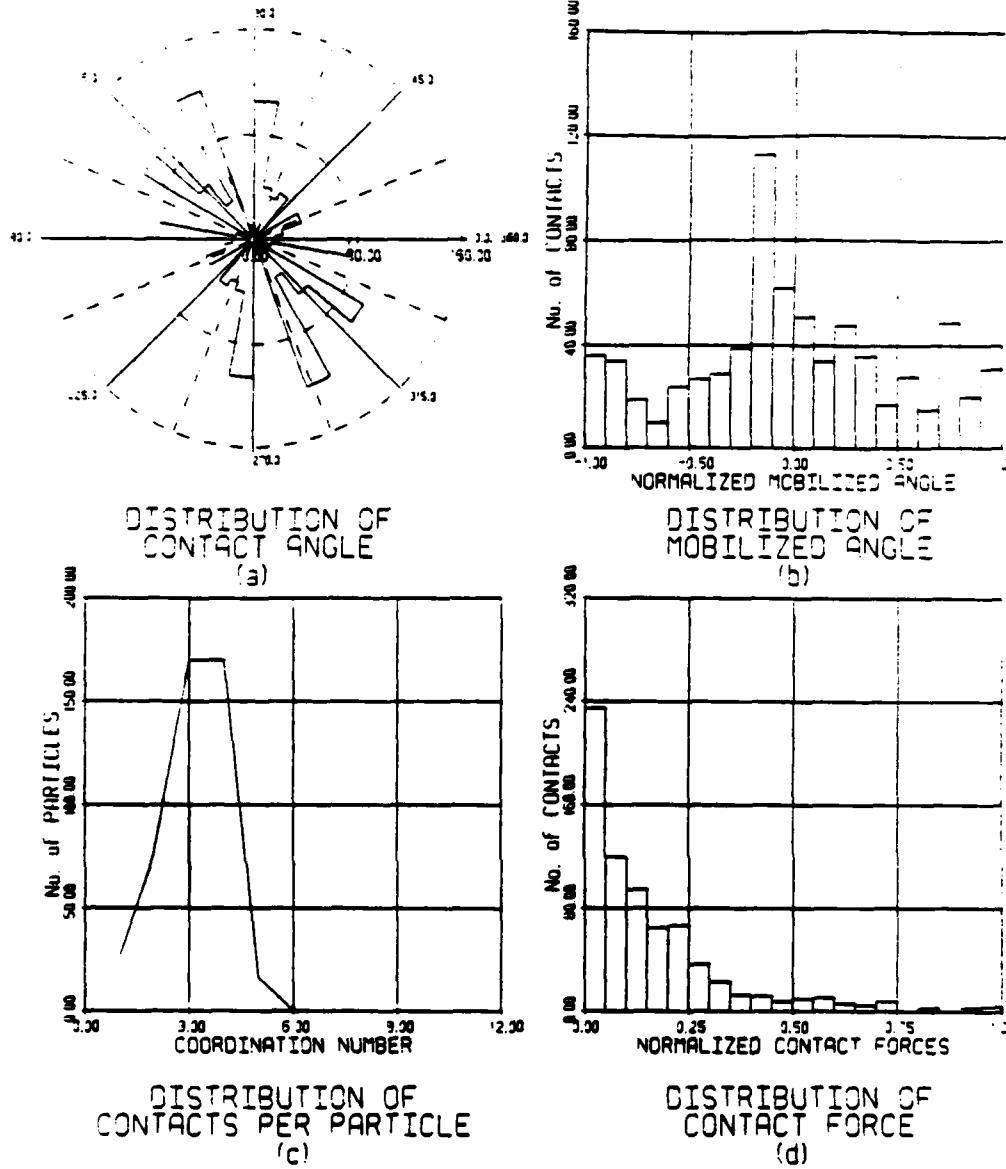
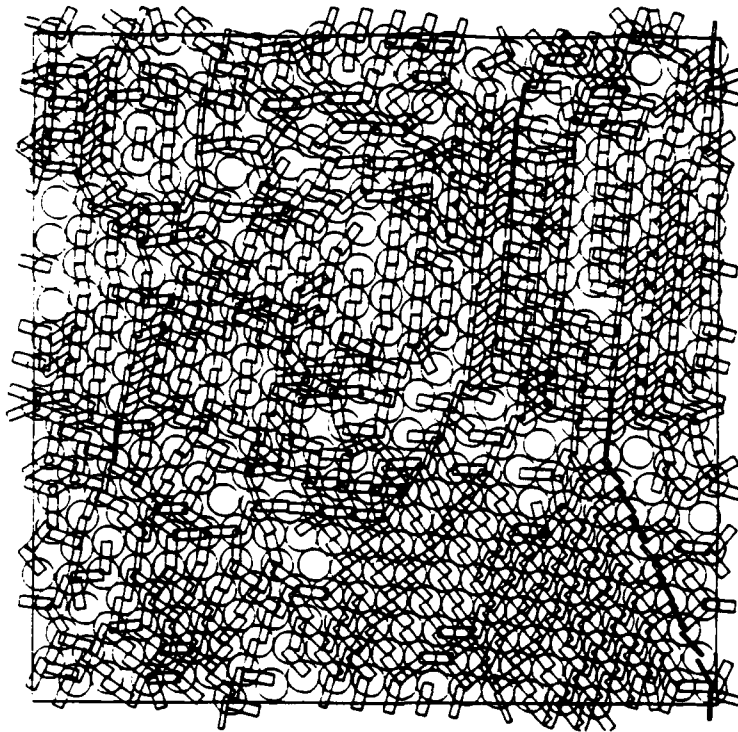
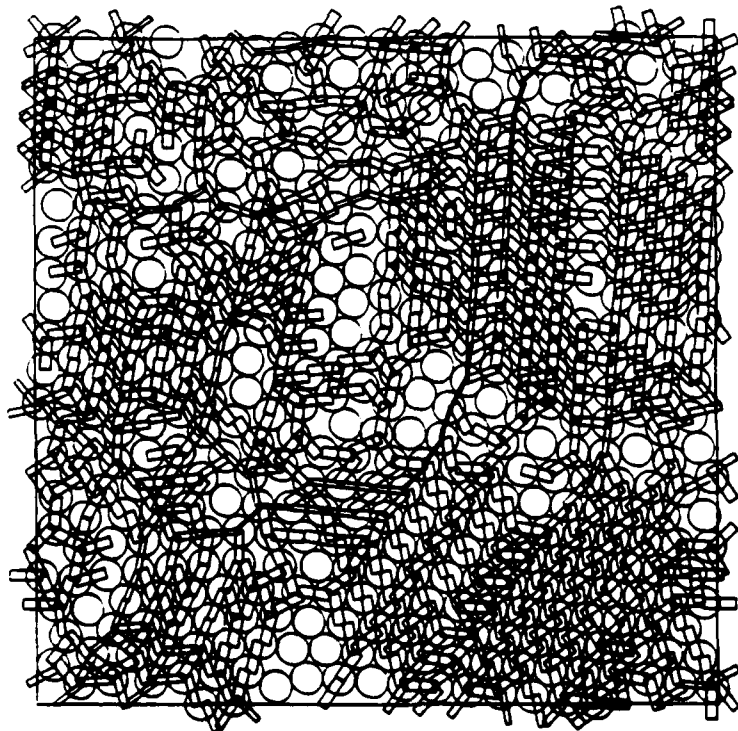


Fig. 20. Statistical Information regarding the state of the 477 particle array of Fig. 4 at point 3 on the yield surface of Fig. 10.



**Fig. 21.** Geometry and contact force distribution of the 477 particle array of Fig. 5 at point 1 on the yield surface of Fig. 10.



**Fig. 22.** Geometry and contact force distribution of the 477 particle array of Fig. 5 at point 2 on the yield surface of Fig. 10.